QCD/QED NONRELATIVISTIC BOUND STATES

FOR THE PRACTITIONER IN THE WEAK COUPLING REGIME

ANTONIO PINEDA

(IFAE, Universitat Autònoma de Barcelona)

Index

Exercise: Compute the positronium (e^+e^-) spectrum to $O(m\alpha^5)$

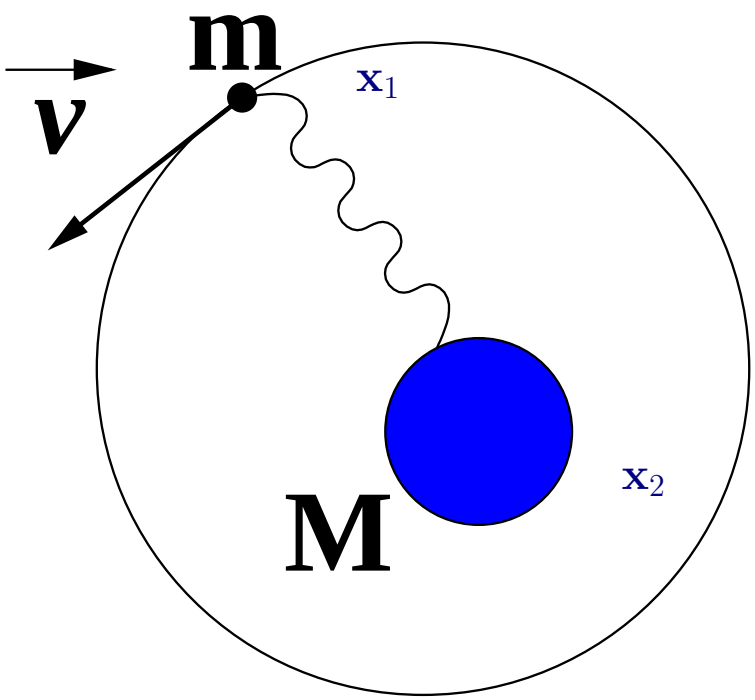

$$H = \frac{\mathbf{p}^2}{2m} + V(r) \qquad V(r) = -\frac{Z_1 Z_2 \alpha}{r}$$

$$v \sim \alpha \ll 1$$

$$\mathbf{x} = \mathbf{x}_1 - \mathbf{x}_2 \qquad \mathbf{X} = \frac{m}{m+M}\mathbf{x}_1 + \frac{M}{m+M}\mathbf{x}_2$$

Scales: m, $m\alpha$, $m\alpha^2$, ...

Motivation

Motivation

Real Motivation: to understand the connection between non-relativistic (NR) Quantum Mechanics and Quantum Field Theories.

Motivation

Real Motivation: to understand the connection between non-relativistic (NR) Quantum Mechanics and Quantum Field Theories.

"Physical Systems":

1) NR bound state systems:

- QED: positronium, Hydrogen-like/exotic atoms, atomic physics ...
- QCD: Heavy Quarkonium (Υ, J/ψ, B_c ...), ...

2) Q-$\bar{Q}$ production near threshold (t-$\bar{t}$ at NLC).

3) Static systems $\leftrightarrow$ lattice "experimental" data.

Motivation

Real Motivation: to understand the connection between non-relativistic (NR) Quantum Mechanics and Quantum Field Theories.

"Physical Systems":

1) NR bound state systems:

- QED: positronium, Hydrogen-like/exotic atoms, atomic physics ...
- QCD: Heavy Quarkonium (Υ, J/ψ, B_c ...), ...

2) Q-$\bar{Q}$ production near threshold (t-$\bar{t}$ at NLC).

3) Static systems $\leftrightarrow$ lattice "experimental" data.

Better understanding of QCD and better determination of the parameters of the Standard Model: m_b, m_t, α_s, m_l, α_{em}, ...}

Motivation

Real Motivation: to understand the connection between non-relativistic (NR) Quantum Mechanics and Quantum Field Theories.

"Physical Systems":

1) NR bound state systems:

- QED: positronium, Hydrogen-like/exotic atoms, atomic physics ...
- QCD: Heavy Quarkonium (Υ, J/ψ, B_c ...), ...

2) Q-$\bar{Q}$ production near threshold (t-$\bar{t}$ at NLC).

3) Static systems $\leftrightarrow$ lattice "experimental" data.

Better understanding of QCD and better determination of the parameters of the Standard Model: m_b, m_t, α_s, m_l, α_{em}, ...}

Tool: **Effective Field Theories $\equiv$ Factorization**

Why?: There is a hierarchy of different scales (hard, soft and ultrasoft).

$$m >> mv >> mv^2\,, \quad (\Lambda_{QCD})$$

EFTs are especially useful in these situations.

1) Perturbative calculations much easier and systematic.

2) Nonperturbative information is parameterized in a model independent way.

3) Power counting.

1.a): kinematical situation

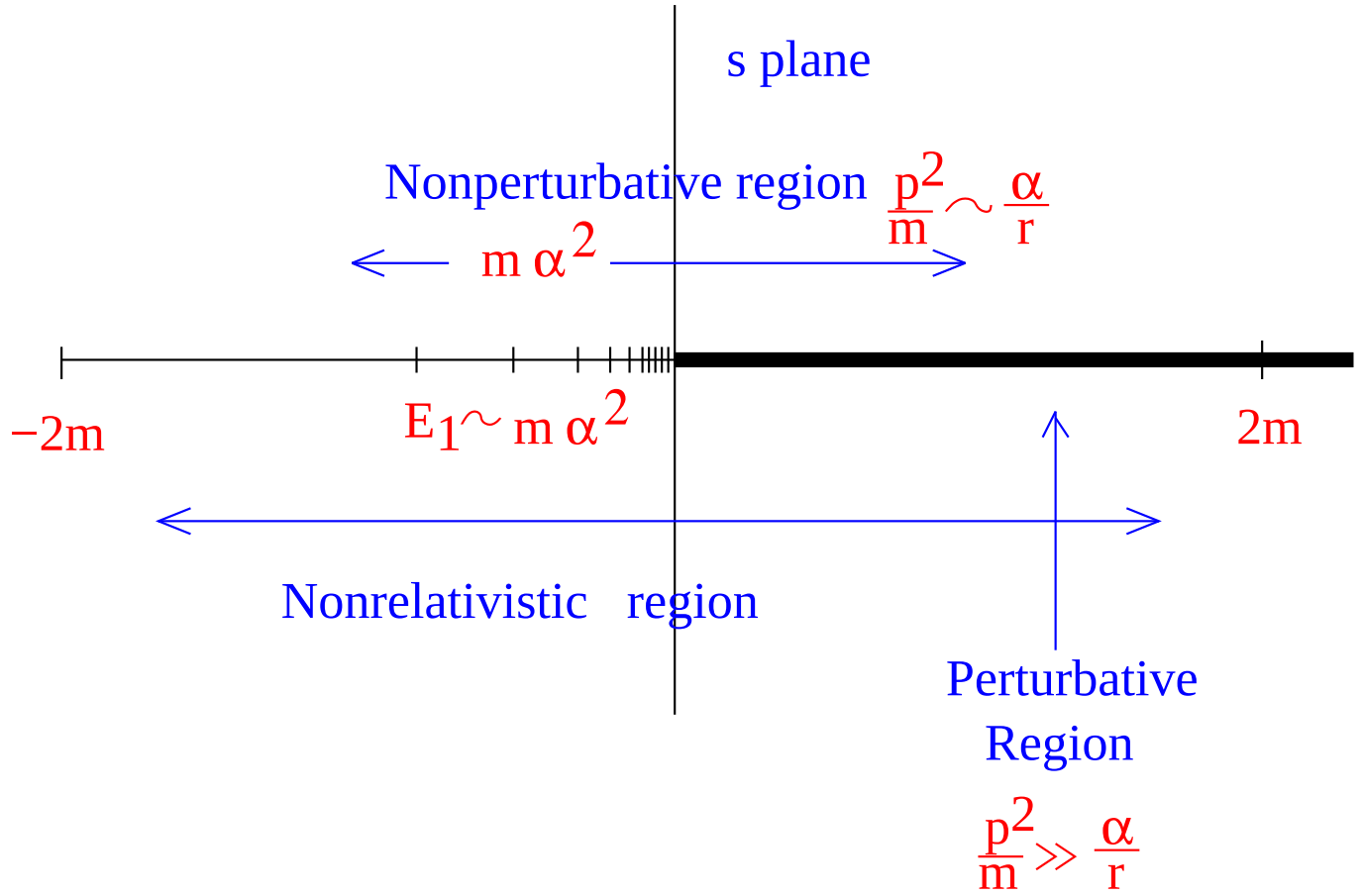

1st approximation: ∞ number of NR (bound states) free particles

Unusual situation in EFTs. What we will get is somewhat unusual from the EFT point of view.

$$\mathcal{L}_{(n)} = \psi_n^\dagger(\mathbf{X},t)(i\partial_0 + \frac{\boldsymbol{\nabla}_X^2}{2M} - E_n + i\epsilon)\psi_n(\mathbf{X},t)$$

Our case

$$\mathcal{L} = \Sigma_n \, \psi_n^\dagger(\mathbf{X}, t)(i\partial_0 + \frac{\boldsymbol{\nabla}_X^2}{2M} - E_n + i\epsilon)\psi_n(\mathbf{X}, t)$$

$\psi_n(\mathbf{X})$ represents the quark-antiquark bound state

Path integral formulation:

$$Z = \int \Pi D\psi_n^\dagger D\psi_n e^{i\int d^4X(\mathcal{L}+\psi_n^\dagger\eta_n+\eta_n^\dagger\psi_n)}$$

Connection with quantum mechanics (?):
particle-antiparticle wave function: $\Psi(\mathbf{X}, \mathbf{x}) = \Psi_{\mathbf{x}}(\mathbf{X})$
$\mathbf{X}$ = Center of mass coordinate
$\mathbf{x}$ = relative coordinate

Ansatz: Promote $\Psi(\mathbf{X}, \mathbf{x})$ to a field

$$Z = \int D\Psi(X, x)^\dagger D\Psi(X, x) e^{i\int d^4X d^3\mathbf{x}(\mathcal{L}+\Psi^\dagger J(X,x)+J^\dagger(X,x)\Psi)}$$

$$\mathcal{L} = \Psi^\dagger(i\partial_0 - \hat{h} + i\epsilon)\Psi$$

where

$$\hat{h} = \hat{h}_{\mathbf{X}} + \hat{h}_{\mathbf{x}}\,, \quad \hat{h}_{\mathbf{X}} = -\frac{\boldsymbol{\nabla}_X^2}{2M}\,, \quad \hat{h}_{\mathbf{x}} = -\frac{\boldsymbol{\nabla}_x^2}{2\mu_r} + V(\mathbf{x})$$

We have traded E_n for $V(\mathbf{x})$. The point is that we will able to relate $V(\mathbf{x})$ with some Green functions in the underlying theory and in some kinematical regime to compute it perturbatively.

Change of basis

$\Psi(\mathbf{X},\mathbf{x}) = \Sigma_n\, \phi_n(\mathbf{x})\psi_n(\mathbf{X})$

where $\phi_n(\mathbf{x})$ is a function and $\psi_n(\mathbf{X})$ a field and

$$\hat{h}_{\mathbf{x}}\phi_n(\mathbf{x}) = E_n\phi_n(\mathbf{x})$$

$$Z = N\int \Pi D\psi_n^\dagger D\psi_n e^{i\int d^4X(\Sigma_n\,\psi_n^\dagger(i\partial_0+\frac{\boldsymbol{\nabla}_X^2}{2M}-E_n+i\epsilon)\psi_n+\int d^3x\,\Sigma_n(\phi_n^*\psi_n^\dagger J+J^\dagger\phi_n\psi_n))}$$

$$\int d^3x\phi_{n'}^*\hat{h}_{\mathbf{x}}\phi_n = \delta_{nn'}E_n$$

$$\int d^3x\phi_{n'}^*\phi_n = \delta_{nn'}$$

We have closed the connection between both formulations

Infinite number of states $\leftrightarrow$ Integro-diferential equation (Schrödinger equation)

NR Effective Field Theories

Our aim is to provide a systematic method to deal with NR bound state systems. We will introduce a hierarchy of EFTs when sequentially integrating out each scale (only one scale in each step, strong simplification).

QCD

↓ Integrating out the hard scale (m)

NRQCD — Caswell, Lepage

↓ Integrating out the soft scale (mv)

pNRQCD — Soto, Pineda

$$\left.\begin{array}{l}\left(i\partial_0 - \dfrac{\mathbf{p}^2}{2m} - V_0(r)\right)\Phi(\mathbf{r}) = 0 \\ +\text{corrections to the potential} \\ +\text{interaction with other low} \\ \quad \text{energy degrees of freedom}\end{array}\right\} \text{potential NRQCD} \qquad E \sim mv^2$$

In the perturbative case the starting point is $V_0 = -C_f \dfrac{\alpha}{r}$.

NRQCD: the scale m

- Degrees of freedom
- Symmetries
- Cutoff

NRQCD has an ultraviolet cutoff Λ such that $m \gg \Lambda$ and larger than any other dynamical scale in the problem. $\Psi = \psi + \chi$

$$\mathcal{L}_{NRQCD} = \bar{\Psi} i\gamma^0 D_0 \Psi + \bar{\Psi}\{\frac{\mathbf{D}^2}{2m} + c_F\, g\frac{\mathbf{\Sigma}\cdot\mathbf{B}}{2m} + c_D\, g\frac{\gamma^0\,(\mathbf{D}\cdot\mathbf{E} - \mathbf{E}\cdot\mathbf{D})}{8m^2}$$
$$+ ic_S\, g\frac{\gamma^0\mathbf{\Sigma}\cdot(\mathbf{D}\times\mathbf{E} - \mathbf{E}\times\mathbf{D})}{8m^2} + \frac{\mathbf{D}^4}{8m^3}\}\Psi$$
$$-\frac{1}{4}c_1 F_{\mu\nu}F^{\mu\nu} + \frac{c_2}{m^2}gF_{\mu\nu}D^2 gF^{\mu\nu} + \frac{c_3}{m^2}g^3 f_{ABC}F^A_{\mu\nu}F^B_{\mu\alpha}F^C_{\nu\alpha}$$

$$\delta\mathcal{L}_{NRQCD} = \frac{d_{ss}}{m_1 m_2}\psi_1^\dagger\psi_1\chi_2^\dagger\chi_2 + \frac{d_{sv}}{m_1 m_2}\psi_1^\dagger\boldsymbol{\sigma}\psi_1\chi_2^\dagger\boldsymbol{\sigma}\chi_2$$
$$+\frac{d_{vs}}{m_1 m_2}\psi_1^\dagger \mathrm{T}^a\psi_1\chi_2^\dagger \mathrm{T}^a\chi_2 + \frac{d_{vv}}{m_1 m_2}\psi_1^\dagger \mathrm{T}^a\boldsymbol{\sigma}\psi_1\chi_2^\dagger \mathrm{T}^a\boldsymbol{\sigma}\chi_2\,.$$

Lepage, Caswell, Thacker

Matching QCD to NRQCD: the scale m

$c_i = 1 + O(\alpha_s)$, $d_1 = 1 + O(\alpha_s^2)$ (relevant α_s at low energies), d_2 ,d_3, d_{ss}, ...$= O(\alpha_s)$.

Typically, $\quad c_i \sim 1 + \alpha_s \left(A \log \frac{m}{\mu} + B \right) \qquad d_i \sim \alpha_s \left(1 + \alpha_s \left(A \log \frac{m}{\mu} + B \right) \right)$

Matching QCD to NRQCD: the scale m

$c_i = 1 + O(\alpha_s)$, $d_1 = 1 + O(\alpha_s^2)$ (relevant α_s at low energies), d_2 ,d_3, d_{ss}, ...$= O(\alpha_s)$.

Typically, $\quad c_i \sim 1 + \alpha_s \left(A \log \frac{m}{\mu} + B \right) \qquad d_i \sim \alpha_s \left(1 + \alpha_s \left(A \log \frac{m}{\mu} + B \right) \right)$

One major problem: Matching QCD to NRQCD with dimensional regularization.

Matching QCD to NRQCD: the scale m

$c_i = 1 + O(\alpha_s)$, $d_1 = 1 + O(\alpha_s^2)$ (relevant α_s at low energies), d_2 ,d_3, d_{ss}, ...$= O(\alpha_s)$.

Typically, $\quad c_i \sim 1 + \alpha_s \left(A \log \frac{m}{\mu} + B \right) \qquad d_i \sim \alpha_s \left(1 + \alpha_s \left(A \log \frac{m}{\mu} + B \right) \right)$

One major problem: Matching QCD to NRQCD with dimensional regularization.
In order to integrate the mass scale it is only needed

$$\boxed{m >> |\mathbf{p}|, E, \Lambda_{QCD}}$$

Matching QCD to NRQCD: the scale m

$c_i = 1 + O(\alpha_s)$, $d_1 = 1 + O(\alpha_s^2)$ (relevant α_s at low energies), d_2 ,d_3, d_{ss}, ...$= O(\alpha_s)$.

Typically, $\quad c_i \sim 1 + \alpha_s \left(A \log \frac{m}{\mu} + B \right) \qquad d_i \sim \alpha_s \left(1 + \alpha_s \left(A \log \frac{m}{\mu} + B \right) \right)$

One major problem: Matching QCD to NRQCD with dimensional regularization.
In order to integrate the mass scale it is only needed

$$\boxed{m >> |\mathbf{p}|, E, \Lambda_{QCD}}$$

One matches to HQET from a practical point of view.

Matching QCD to NRQCD: the scale m

$c_i = 1 + O(\alpha_s)$, $d_1 = 1 + O(\alpha_s^2)$ (relevant α_s at low energies), d_2 ,d_3, d_{ss}, ...$= O(\alpha_s)$.

Typically, $\quad c_i \sim 1 + \alpha_s \left(A \log \frac{m}{\mu} + B \right) \qquad d_i \sim \alpha_s \left(1 + \alpha_s \left(A \log \frac{m}{\mu} + B \right) \right)$

One major problem: Matching QCD to NRQCD with dimensional regularization.
In order to integrate the mass scale it is only needed

$$\boxed{m >> |\mathbf{p}|, E, \Lambda_{QCD}}$$

One matches to HQET from a practical point of view.

Analytical expansion over the three-momentum and residual energy in the integrand before the integration is made in both the full and the effective theory.

QCD

$$\int d^4q f(q, m, |\mathbf{p}|, E) = \int d^4q f(q, m, 0, 0) + O\left(\frac{E}{m}, \frac{|\mathbf{p}|}{m}\right)$$

NRQCD

$$\int d^4q f(q, |\mathbf{p}|, E) = \int d^4q f(q, 0, 0) = 0 \,!!$$

Dimensional regularization. The computation of loops in the effective theory just gives zero.

Final rules:

- QCD tree level Feynman diagrams $\longrightarrow$ non-relativistic reduction. They give the leading contribution to the NRQCD matching coefficients (this is equivalent to perform a Foldy-Wouthysen transformation for the bilinear piece of the Lagrangian but not for four-fermion operators due to the annihilation terms).
- One matches loops in QCD with only one scale (the mass) to tree level diagrams in NRQCD.
- Matching to some given order in α and $1/m$, i.e. to $O(\alpha^n/m^s)$.

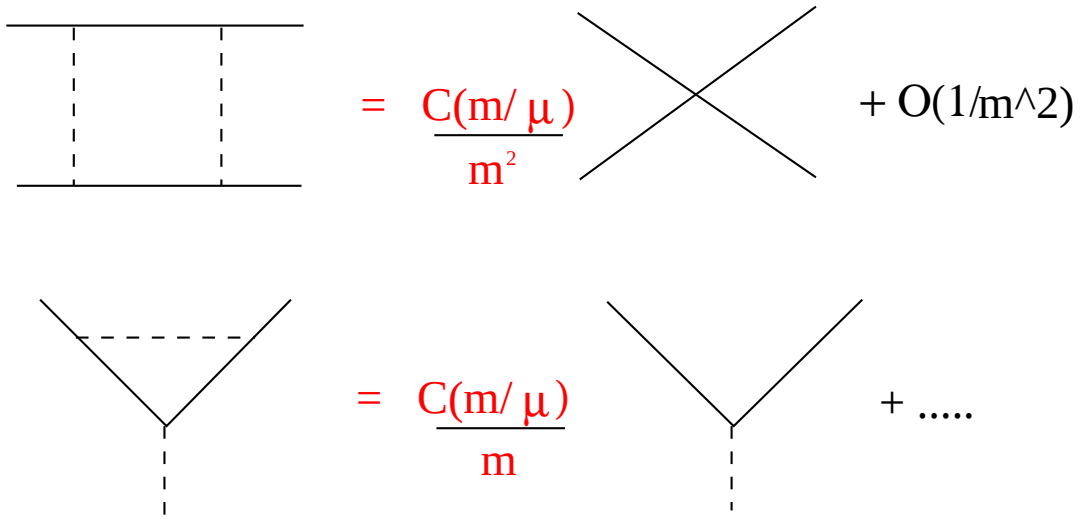

Manohar; Soto, Pineda

Other problem. Power counting of NRQCD in the perturbative situation.

Other problem. Power counting of NRQCD in the perturbative situation.
Previous work: Labelle $\longrightarrow$ Multipole expansion (QED)
Manohar, Luke; Grinstein, Rothstein; Savage, Luke

Other problem. Power counting of NRQCD in the perturbative situation.
Previous work: Labelle $\longrightarrow$ Multipole expansion (QED)
Manohar, Luke; Grinstein, Rothstein; Savage, Luke
Next step:
Soto, Pineda$\longrightarrow$How would we like the effective theory for Q–$\bar{Q}$ systems near threshold to be?
We do not want to describe all the degrees of freedom included in NRQCD, but rather only those with US energy. Moreover, we want to get a closer connection with a Schrödinger-like formulation for these systems (also, eventually, in the non-perturbative regime $\longrightarrow$ potential models). We will call potential NRQCD this new effective theory.

Other problem. Power counting of NRQCD in the perturbative situation.
Previous work: Labelle $\longrightarrow$ Multipole expansion (QED)
Manohar, Luke; Grinstein, Rothstein; Savage, Luke
Next step:
Soto, Pineda$\longrightarrow$How would we like the effective theory for Q–$\bar{Q}$ systems near threshold to be?
We do not want to describe all the degrees of freedom included in NRQCD, but rather only those with US energy. Moreover, we want to get a closer connection with a Schrödinger-like formulation for these systems (also, eventually, in the non-perturbative regime $\longrightarrow$ potential models). We will call potential NRQCD this new effective theory.
Beneke, Smirnov$\longrightarrow$ threshold expansion. Rigorous diagrammatic study of the (perturbative) momentum regions: hard, soft, potential, ultrasoft.
hard: particles with $E \sim |\mathbf{p}| \sim m \longrightarrow$ NRQCD
soft: particles with $E \sim |\mathbf{p}| \sim mv \longrightarrow$ pNRQCD
potential: particles with $E \sim mv^2$, $|\mathbf{p}| \sim mv$
ultrasoft: particles with $E \sim |\mathbf{p}| \sim mv^2$
Implementation of pNRQCD through the threshold expansion (integrating out potential gluons and all soft particles): Beneke, Smirnov; Kniehl, Penin; Kniehl, Penin, Smirnov, Steinhauser

Physical Picture

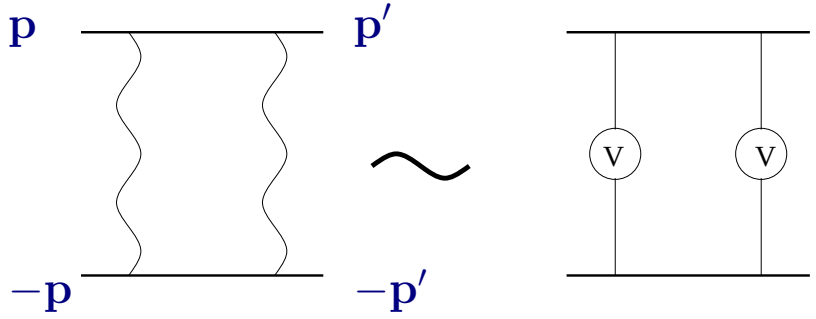

$$I \sim \int \frac{d^4 q}{(2\pi)^4} V(p,q) \frac{1}{E/2 + q^0 - \mathbf{q}^2/2m + i\epsilon} \frac{1}{E/2 - q^0 - \mathbf{q}^2/2m + i\epsilon} V(q,p')$$

$$V(p,q) \sim \frac{1}{(p-q)^2}$$

Counting (different possibilities):

A) $E \sim mv^2 \quad p^0, p'^0 \sim q^0 \sim |\mathbf{p}| \sim \mathbf{q} \sim \mathbf{p}' \sim mv$

Static propagator:

$$\frac{i}{q^0 + i\epsilon}$$

B) $E \sim p^0, p'^0 \sim q^0 \sim mv^2 \quad |\mathbf{p}| \sim \mathbf{q} \sim \mathbf{p}' \sim mv$

Nonrelativistic propagator:

$$\frac{i}{q^0 - \mathbf{q}^2/(2m) + i\epsilon}$$

Leading contribution:

$$I \sim \int \frac{d^3\,\mathbf{q}}{(2\pi)^3} V(\mathbf{p},\mathbf{q}) \frac{1}{E - \mathbf{q}^2/m + i\epsilon} V(\mathbf{q},\mathbf{p}')\,.$$

But this is nothing but the usual NR Quantum Mechanics!!, I can be written as

$$I \sim \langle \mathbf{p}|\hat{V} \frac{1}{E - \hat{\mathbf{p}}^2/m + i\epsilon} \hat{V}|\mathbf{p}'\rangle$$

In fact, this can be done to any order considering ladder loops. Therefore, we obtain that the QFT amplitude can be written (within this approximation) as the Quantum Mechanical one

$$i\mathcal{A} = -i\langle \mathbf{p}| \left(\hat{V} + \hat{V} \frac{1}{E - \hat{\mathbf{p}}^2/m + i\epsilon} \hat{V} + \ldots \right) |\mathbf{p}'\rangle\,.$$

For the bound state $V \sim E \sim mv^2$, $p \sim mv$ and one has to sum up the whole series.

pNRQCD: the scale mv

The integration of the mv scale gives rise to potential terms. The Lagrangian is local in time but not in space.

Playing with the scales:

1) $mv \sim \Lambda_{QCD}$

2) $mv \gg \Lambda_{QCD} \gg mv^2$

3) $mv \gg mv^2 \sim \Lambda_{QCD}$

4) $mv \gg mv^2 \gg \Lambda_{QCD}$

Loosely speaking, when to trust the perturbative calculation and the size of NP corrections.

$\boxed{mv \gg \Lambda_{QCD}}$ ($\Upsilon(1S)$, t-$\bar{t}$, b-$\bar{b}$ sum rules)

- Degrees of freedom
- symmetries
- cutoff

pNRQCD has two ultraviolet cut-offs, ν_{us} and ν_p. ν_{us} fulfils the relation $\mathbf{p}^2/m \ll \nu_{us} \ll |\mathbf{p}|$ and is the cut-off of the energy of the quarks, and of the energy and the momentum of the gluons. ν_p fulfils $|\mathbf{p}| \ll \nu_p \ll m$ and is the cut-off of the relative momentum of the quark–antiquark system, $\mathbf{p}$.

Power counting/scales

Scales: m, p, $1/r$, $\Lambda_{mp} = \{\Lambda_{QCD},\, mv^2, ...\}$

Dimensionless quantities:

$$\frac{p}{m},\ \alpha_s,\ \frac{1}{m\,r},\ \boxed{\Lambda_{mp} r} \ll 1$$

The multipole expansion can be used in the new EFT.

Power counting/scales

Scales: m, p, $1/r$, $\Lambda_{mp} = \{\Lambda_{QCD}, mv^2, ...\}$

Dimensionless quantities:

$$\frac{p}{m},\ \alpha_s,\ \frac{1}{m\,r},\ \boxed{\Lambda_{mp} r} \ll 1$$

The multipole expansion can be used in the new EFT.

$$L_{pNRQCD} = L'_{NRQCD} + \int\int d^3x_1 d^3x_2 \psi(x_1)\chi_c(x_2)V(x_1 - x_2)\psi^\dagger(x_1)\chi_c^\dagger(x_2)$$

L'_{NRQCD}, gluons multipole expanded (only ultrasoft gluons).

Power counting/scales

Scales: m, p, $1/r$, $\Lambda_{mp} = \{\Lambda_{QCD},\, mv^2, ...\}$

Dimensionless quantities:

$$\frac{p}{m},\ \alpha_s,\ \frac{1}{m\,r},\ \boxed{\Lambda_{mp} r} \ll 1$$

The multipole expansion can be used in the new EFT.

$$L_{pNRQCD} = L'_{NRQCD} + \int\int d^3x_1 d^3x_2 \psi(x_1)\chi_c(x_2) V(x_1 - x_2)\psi^\dagger(x_1)\chi_c^\dagger(x_2)$$

L'_{NRQCD}, gluons multipole expanded (only ultrasoft gluons).

$$V_s^{(0)} \equiv -C_F \frac{\alpha_{V_s}}{r}.$$

$$\frac{V_s^{(1)}}{m} \equiv -\frac{C_F C_A D_s^{(1)}}{2mr^2}.$$

$$\begin{aligned}\frac{V_s^{(2)}}{m^2} = & -\frac{C_F D_{1,s}^{(2)}}{2m^2}\left\{\frac{1}{r}, \mathbf{p}^2\right\} + \frac{C_F D_{2,s}^{(2)}}{2m^2}\frac{1}{r^3}\mathbf{L}^2 + \frac{\pi C_F D_{d,s}^{(2)}}{m^2}\delta^{(3)}(\mathbf{r}) \\ & + \frac{4\pi C_F D_{S^2,s}^{(2)}}{3m^2}\mathbf{S}^2\delta^{(3)}(\mathbf{r}) + \frac{3C_F D_{LS,s}^{(2)}}{2m^2}\frac{1}{r^3}\mathbf{L}\cdot\mathbf{S} + \frac{C_F D_{S_{12},s}^{(2)}}{4m^2}\frac{1}{r^3}S_{12}(\hat{\mathbf{r}}),\end{aligned}$$

where $S_{12}(\hat{\mathbf{r}}) \equiv 3\hat{\mathbf{r}}\cdot\boldsymbol{\sigma}_1\,\hat{\mathbf{r}}\cdot\boldsymbol{\sigma}_2 - \boldsymbol{\sigma}_1\cdot\boldsymbol{\sigma}_2$ and $\mathbf{S} = \boldsymbol{\sigma}_1/2 + \boldsymbol{\sigma}_2/2$.

To go to the wave function description one has to project to the quark-antiquark sector.

$$\int d^3\mathbf{x}_1 d^3\mathbf{x}_2 \Psi(\mathbf{x}_1,\mathbf{x}_2)\psi(x_1)\chi_c(x_2)|0\rangle$$

$$H\int d^3\mathbf{x}_1 d^3\mathbf{x}_2 \Psi(\mathbf{x}_1,\mathbf{x}_2)\psi^\dagger(\mathbf{x}_1)\chi_c^\dagger(\mathbf{x}_2)|0\rangle = \int d^3\mathbf{x}_1 d^3\mathbf{x}_2 (\hat{h}\Psi(\mathbf{x}_1,\mathbf{x}_2))\psi^\dagger(\mathbf{x}_1)\chi_c^\dagger(\mathbf{x}_2)|0\rangle$$

To go to the wave function description one has to project to the quark-antiquark sector.

$$\int d^3\mathbf{x}_1 d^3\mathbf{x}_2 \Psi(\mathbf{x}_1,\mathbf{x}_2)\psi(x_1)\chi_c(x_2)|0\rangle$$

$$H\int d^3\mathbf{x}_1 d^3\mathbf{x}_2 \Psi(\mathbf{x}_1,\mathbf{x}_2)\psi^\dagger(\mathbf{x}_1)\chi_c^\dagger(\mathbf{x}_2)|0\rangle = \int d^3\mathbf{x}_1 d^3\mathbf{x}_2 (\hat{h}\Psi(\mathbf{x}_1,\mathbf{x}_2))\psi^\dagger(\mathbf{x}_1)\chi_c^\dagger(\mathbf{x}_2)|0\rangle$$

For QED

$$\begin{aligned} L_{pNRQED} &= \int d^3\mathbf{x}_1 d^3\mathbf{x}_2 \Psi^\dagger(\mathbf{x}_1,\mathbf{x}_2)(iD_0 + \frac{\mathbf{D}^2_{\mathbf{x}_1}}{2m_1} + \frac{\mathbf{D}^2_{\mathbf{x}_2}}{2m_2} - V(\mathbf{x},\mathbf{p}))\Psi(\mathbf{x}_1,\mathbf{x}_2) \\ &= \int d^3\mathbf{x}_1 d^3\mathbf{x}_2 \Psi^\dagger(\mathbf{x}_1,\mathbf{x}_2)(i\partial_0 + \frac{\boldsymbol{\nabla}^2_{\mathbf{x}}}{m} + \frac{\boldsymbol{\nabla}^2_{\mathbf{X}}}{4m} \\ &\quad -e\mathbf{x}\cdot\boldsymbol{\nabla}A_0(\mathbf{X}) - 2ie\frac{\mathbf{A}(\mathbf{X})\cdot\boldsymbol{\nabla}_{\mathbf{x}}}{m} - V(\mathbf{x},\mathbf{p}))\Psi(\mathbf{x}_1,\mathbf{x}_2) \end{aligned}$$

To go to the wave function description one has to project to the quark-antiquark sector.

$$\int d^3\mathbf{x}_1 d^3\mathbf{x}_2 \Psi(\mathbf{x}_1,\mathbf{x}_2)\psi(x_1)\chi_c(x_2)|0\rangle$$

$$H\int d^3\mathbf{x}_1 d^3\mathbf{x}_2 \Psi(\mathbf{x}_1,\mathbf{x}_2)\psi^\dagger(\mathbf{x}_1)\chi_c^\dagger(\mathbf{x}_2)|0\rangle = \int d^3\mathbf{x}_1 d^3\mathbf{x}_2 (\hat{h}\Psi(\mathbf{x}_1,\mathbf{x}_2))\psi^\dagger(\mathbf{x}_1)\chi_c^\dagger(\mathbf{x}_2)|0\rangle$$

For QED

$$\begin{aligned} L_{pNRQED} &= \int d^3\mathbf{x}_1 d^3\mathbf{x}_2 \Psi^\dagger(\mathbf{x}_1,\mathbf{x}_2)(iD_0 + \frac{\mathbf{D}^2_{\mathbf{x}_1}}{2m_1} + \frac{\mathbf{D}^2_{\mathbf{x}_2}}{2m_2} - V(\mathbf{x},\mathbf{p}))\Psi(\mathbf{x}_1,\mathbf{x}_2) \\ &= \int d^3\mathbf{x}_1 d^3\mathbf{x}_2 \Psi^\dagger(\mathbf{x}_1,\mathbf{x}_2)(i\partial_0 + \frac{\boldsymbol{\nabla}^2_{\mathbf{x}}}{m} + \frac{\boldsymbol{\nabla}^2_{\mathbf{X}}}{4m} \\ &\quad -e\mathbf{x}\cdot\boldsymbol{\nabla}A_0(\mathbf{X}) - 2ie\frac{\mathbf{A}(\mathbf{X})\cdot\boldsymbol{\nabla}_{\mathbf{x}}}{m} - V(\mathbf{x},\mathbf{p}))\Psi(\mathbf{x}_1,\mathbf{x}_2) \end{aligned}$$

New fields: Singlet S, Octet (O) and US gluons.
Gauge transformation:

$$S(\mathbf{x},\mathbf{X},t) \to S(\mathbf{x},\mathbf{X},t)\,, \qquad O(\mathbf{x},\mathbf{X},t) \to g(\mathbf{X},t)O(\mathbf{x},\mathbf{X},t)g^{-1}(\mathbf{X},t)\,.$$

Field Redefinitions.

$$\Psi(\mathbf{x}_1,\mathbf{x}_2) = \phi(\mathbf{x}_1,\mathbf{x}_2)S(\mathbf{x},\mathbf{X}) + \phi(\mathbf{x}_1,\mathbf{X})O(\mathbf{x},\mathbf{X})\phi(\mathbf{X},\mathbf{x}_2)$$

$$\phi(\mathbf{y},\mathbf{x},t) \equiv \mathrm{P}\exp\left\{ig\int_0^1 ds\,(\mathbf{y}-\mathbf{x})\cdot\mathbf{A}(\mathbf{x}-s(\mathbf{x}-\mathbf{y}),t)\right\}$$

pNRQCD Lagrangian at $O(r)$

$$\begin{aligned}
\mathcal{L}_{pNRQCD} &= \mathrm{Tr}\{S^\dagger \left(i\partial_0 - V_s^{(0)}(\mathbf{x})\right) S + O^\dagger \left(iD_0 - V_o^{(0)}(\mathbf{x})\right) O\} \\
&+ g V_A(\mathbf{x}) \mathrm{Tr}\left\{O^\dagger \mathbf{x}\cdot\mathbf{E}\, S + S^\dagger \mathbf{x}\cdot\mathbf{E}\, O\right\} + g\frac{V_B(\mathbf{x})}{2}\mathrm{Tr}\left\{O^\dagger \mathbf{x}\cdot\mathbf{E}\, O + O^\dagger O \mathbf{x}\cdot\mathbf{E}\right\} \\
&- \mathrm{Tr}\{S^\dagger \left(\frac{\mathbf{p}^2}{m} + \sum_n \frac{V_s^{(n)}(\mathbf{x})}{m^n}\right) S - O^\dagger \left(\frac{\mathbf{p}^2}{m} + \sum_n \frac{V_o^{(n)}(\mathbf{x})}{m^n}\right) O\},
\end{aligned}$$

Interpolating fields:

$$Q_2^\dagger(\mathbf{x}_2,t)\phi(\mathbf{x}_2,\mathbf{x}_1;t)Q_1(\mathbf{x}_1,t) = Z_s^{1/2}(\mathbf{x})S(\mathbf{X},\mathbf{x},t)$$

$$Q_2^\dagger(x_2)\phi(\mathbf{x}_2,\mathbf{X};t)T^a\phi(\mathbf{X},\mathbf{x}_1;t)Q_1(x_1) = Z_o^{1/2}(\mathbf{x})O^a(\mathbf{X},\mathbf{x},t)$$

Matching NRQCD to pNRQCD

Same idea than in NRQCD. Expansion in the scales that are left in the effective theory. We integrate out the scale k (transfer momentum between the quark and antiquark).
Analytical expansion of $\mathbf{1/m}$ (and therefore $\mathbf{p}$) and $\mathbf{E}$ before the integration is made in both the full and the effective theory. Effectively HQET-like rules (HQET quark propagator).
NRQCD

$$\int d^4q f(q,k,|\mathbf{p}|,E) = \int d^4q f(q,k,0,0) + O\left(\frac{E}{k},\frac{|\mathbf{p}|}{k}\right) \qquad \text{potentials}$$

pNRQCD

$$\int d^4q f(q,|\mathbf{p}|,E) = \int d^4q f(q,0,0) = 0\,!!$$

Dimensional regularization. The computation in the effective theory just gives zero.

Final rules:

- NRQCD tree level Feynman diagrams $\longrightarrow$ non-relativistic reduction. They give the leading contribution to the potentials.
- One matches loops in NRQCD with only one scale (k) to tree level diagrams in pNRQCD (potentials).
- Matching to some given order in α and $1/m$, i.e. $O(\alpha^n/m^s)$.

It can also be understood within the threshold expansion: integrating out potential gluons and soft particles.

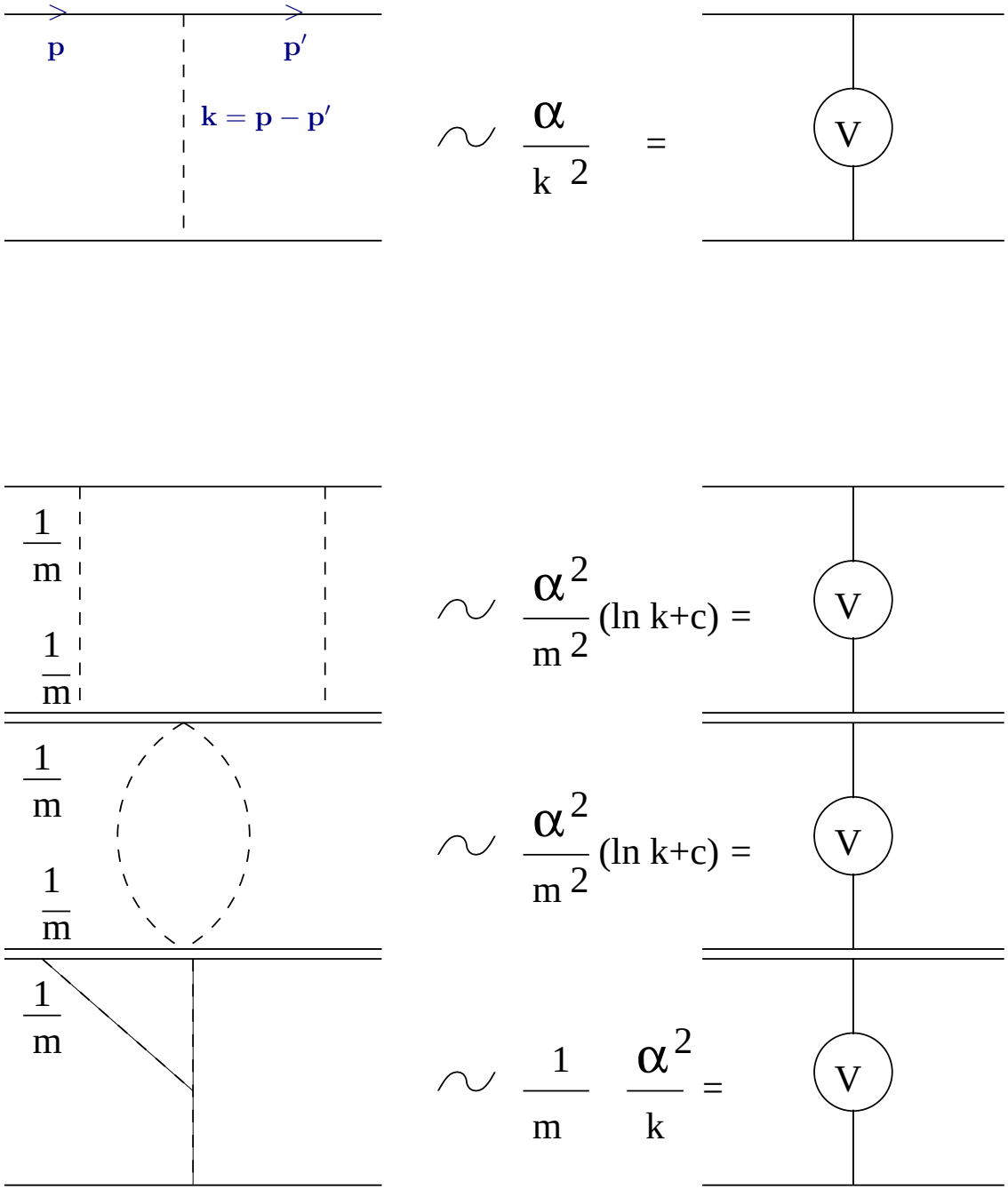
p
p′
k = p − p′
∼ α / k 2 =
V
1/m
1/m
∼ α 2 / m 2 (ln k+c) =
V
1/m
1/m
∼ α 2 / m 2 (ln k+c) =
V
1/m
∼ 1/m α 2 / k =
V
NRQCD
pNRQCD

$$\alpha_{V_s} = \alpha_{\rm s}(r)\left\{1 + (a_1 + 2\gamma_E\beta_0)\,\frac{\alpha_{\rm s}(r)}{4\pi} + \left[\gamma_E\,(4a_1\beta_0 + 2\beta_1) + \left(\frac{\pi^2}{3} + 4\gamma_E^2\right)\beta_0^2 + a_2\right]\frac{\alpha_{\rm s}^2(r)}{16\,\pi^2}\right.$$
$$\left. + \frac{C_A^3}{12}\frac{\alpha_{\rm s}^3}{\pi}\ln\mu r\right\}, \quad (a_2,\ \text{Schroeder},\ \text{Peter})$$

$$D_s^{(1)} = \alpha_{\rm s}^2(r)\left\{1 + \frac{2}{3}(4C_F + 2C_A)\frac{\alpha_s}{\pi}\ln\mu r\right\},$$

$$D_{1,s}^{(2)} = \alpha_{\rm s}(r)\left\{1 + \frac{4}{3}C_A\frac{\alpha_s}{\pi}\ln\mu r\right\},$$

$$D_{2,s}^{(2)} = \alpha_{\rm s}(r),$$

$$D_{d,s}^{(2)} = \alpha_{\rm s}(r)\left\{1 + \frac{\alpha_s}{\pi}\left(\frac{2C_F}{3} + \frac{17C_A}{3}\right)\ln mr + \frac{16}{3}\frac{\alpha_s}{\pi}\left(\frac{C_A}{2} - C_F\right)\ln\mu r\right\},$$

$$D_{S^2,s}^{(2)} = \alpha_s(r)\left\{1 - \frac{7C_A}{4}\frac{\alpha_s}{\pi}\ln mr\right\},$$

$$D_{LS,s}^{(2)} = \alpha_s(r)\left\{1 - \frac{2C_A}{3}\frac{\alpha_s}{\pi}\ln mr\right\},$$

$$D_{S_{12},s}^{(2)} = \alpha_s(r)\left\{1 - C_A\frac{\alpha_s}{\pi}\ln mr\right\}.$$

Previous work: Gupta, Radford, Repko; Titard, Ynduráin

Logs: Brambilla, Soto, Vairo, Pineda; Kniehl, Penin; Hoang, Manohar Stewart

Finite terms $1/m$ and $1/m^2$ potentials: Kniehl, Penin, Smirnov, Steinhauser

Renormalization group improved expressions: Soto, Pineda; Pineda

Another possibility: to perform directly the matching to singlet and octet fields, one naturally ends up with Wilson loops.

Expansion in $1/M$. HQET can be used in the matching (static sources).

A) Wilson loop formalism. Suitable if we can not work perturbatively. For example, the computation of the following Green function in both theories

$$\langle 0|Q_2^\dagger(x_2)\phi(x_2,x_1)Q_1(x_1)Q_1^\dagger(y_1)\phi(y_1,y_2)Q_2(y_2)|0\rangle,$$

NRQCD

$$\delta^3(\mathbf{x}_1-\mathbf{y}_1)\delta^3(\mathbf{x}_2-\mathbf{y}_2)\langle W_\square\rangle,$$

pNRQCD

$$Z_s(\mathbf{r})\delta^3(\mathbf{x}_1-\mathbf{y}_1)\delta^3(\mathbf{x}_2-\mathbf{y}_2)e^{-iTV_s^{(0)}(\mathbf{r})}$$

One obtains:

$$V^{(0)}(\mathbf{r})=\lim_{T\to\infty}\frac{i}{T}\log\langle W_\square\rangle=-C_f\frac{\alpha_s}{r}+O(\alpha_s^2)\quad \text{Wilson, Susskind}$$

$$V^{(1,0)}=-\lim_{T\to\infty}\int_0^T dt\,\frac{t}{2}\langle\!\langle g\mathbf{E}_1(t)\cdot g\mathbf{E}_1(0)\rangle\!\rangle_c=-C_fC_A\frac{\alpha_s^2}{4r^2}+O(\alpha_s^3)\ \text{Brambilla, Soto, Vairo, P.}$$

and $O(1/m^2)$ ...

B) Even another method to get the potentials in terms of Wilson loops. Comparison between states and matrix elements in NRQCD and pNRQCD starting from the static solution. Closer in philosophy, and to some extent in the procedure, to standard quantum mechanics perturbation theory.

$\boxed{\Lambda_{QCD} \lesssim mv^2}$ ($\Upsilon(1S)$, b-$\bar{b}$ sum rules, t-$\bar{t}$)

At leading order the Hamiltonian reads ($v \sim C_f \alpha_s/n$)

$$H = H_{Q\bar{Q}} + H_g \,,$$

$$H_{Q\bar{Q}} = P_s H_s + P_o H_o \,, \qquad H_s = -\frac{\Delta}{m} - \frac{C_f \tilde{\alpha}_s(\mu)}{r} \,, \quad H_o = -\frac{\Delta}{m} + \frac{1}{2N_c}\frac{\tilde{\alpha}_s(\mu)}{r} \,,$$

P_s (P_o) is the singlet (octet) projector on a quark-antiquark pair, H_g acts on the gluonic and light quark degrees of freedom. The leading spectra is composed by color singlet Coulomb type bound states

$$M(n,l) = 2m - \frac{m C_f^2 \tilde{\alpha}^2}{4n^2}$$

Corrections:. Perturbative. Expansion in $1/M$, α and the multipole expansion. The leading interaction with ultrasoft gluons reads

$$H_I = -\frac{g}{2}\xi^a \mathbf{x} \cdot \mathbf{E}^a(0) \,,$$

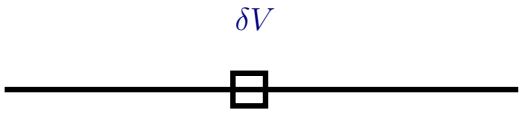

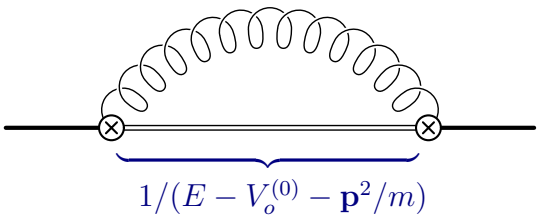

Corrections to the Green Function

$$G_s(E) = P_s \frac{1}{H - H_I - E} P_s = G_s^{(0)} + \delta G_s$$

From the potential:

$$h_s = c_k \frac{\mathbf{p}^2}{m} - C_f \frac{\alpha_{V_s}}{r} - c_4 \frac{\mathbf{p}^4}{4m^3} - \frac{C_f C_A D_s^{(1)}}{2mr^2} - \frac{C_f D_{1,s}^{(2)}}{2m^2} \left\{ \frac{1}{r}, \mathbf{p}^2 \right\} + \frac{C_f D_{2,s}^{(2)}}{2m^2} \frac{1}{r^3} \mathbf{L}^2$$
$$+ \frac{\pi C_f D_{d,s}^{(2)}}{m^2} \delta^{(3)}(\mathbf{r}) + \frac{4\pi C_f D_{S^2,s}^{(2)}}{3m^2} \mathbf{S}^2 \delta^{(3)}(\mathbf{r}) + \frac{3 C_f D_{LS,s}^{(2)}}{2m^2} \frac{1}{r^3} \mathbf{L} \cdot \mathbf{S} + \frac{C_f D_{S_{12},s}^{(2)}}{4m^2} \frac{1}{r^3} S_{12}(\hat{\mathbf{r}}) \,,$$

where $C_f = (N_c^2 - 1)/(2N_c)$ and $c_k = c_4 = 1$ (we only use c_4 for tracking of the contribution due to this term). The propagator of the singlet is (formally)

$$\frac{1}{E - h_s} \,.$$

At leading order (within an strict expansion in α_s) the propagator of the singlet reads

$$= G_c(E) = \frac{1}{E - h_s^{(0)}} = \frac{1}{E - \mathbf{p}^2/m - C_f \alpha_s / r} \,.$$

$$\delta G_s \sim \frac{1}{h_s^{(0)} - E} \delta V \frac{1}{h_s^{(0)} - E}$$

If we were interested in computing the spectrum at $O(m\alpha_s^6)$, one should consider the iteration of subleading potentials (δh_s) in the propagator as follows:

$$G_c(E) \delta h_s G_c(E) \cdots \delta h_s G_c(E) \,.$$

In general, these contributions will produce logarithmic divergences due to potential loops. These divergences can be absorbed in the matching coefficients, $D^{(2)}_{d,s}$ and $D^{(2)}_{S^2,s}$, of the local potentials (proportional to the $\delta^{(3)}(\mathbf{r})$) providing with the renormalization group equations of these matching coefficients in terms of ν_p. Let us explain how it works in detail. Since the singular behavior of the potential loops appears for $\mathbf{p}^2/m \gg \alpha_s/r$, a perturbative expansion in α_s is licit in $G_c(E)$, which can be approximated by

$$= G_c^{(0)}(E) = \frac{1}{E - \mathbf{p}^2/m}\,.$$

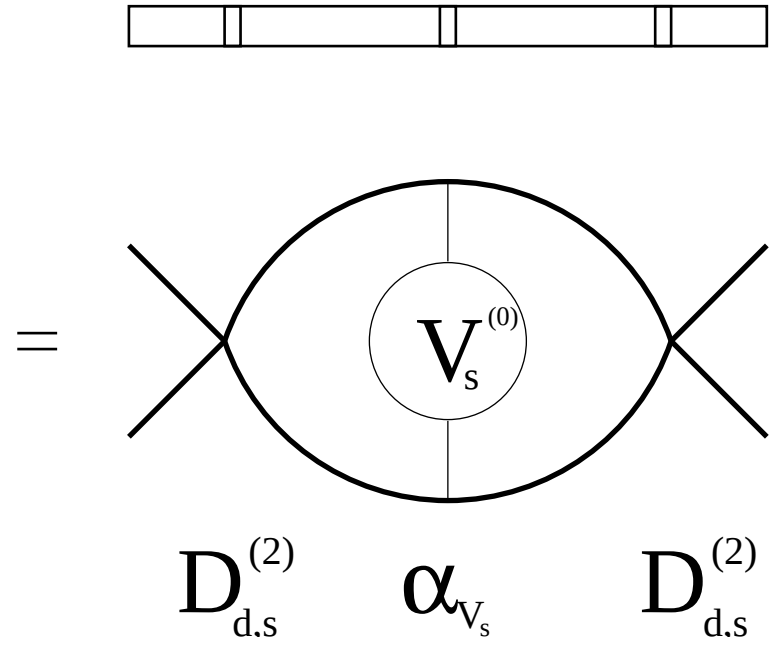

$$\langle \mathbf{r}=0|\frac{1}{E-\mathbf{p}^2/m}C_f\frac{\alpha_{V_s}}{r}\frac{1}{E-\mathbf{p}^2/m}|\mathbf{r}=0\rangle$$
$$\sim \int\frac{\mathrm{d}^d p'}{(2\pi)^d}\int\frac{\mathrm{d}^d p}{(2\pi)^d}\frac{m}{\mathbf{p}'^2-mE}C_f\frac{4\pi\alpha_{V_s}}{\mathbf{q}^2}\frac{m}{\mathbf{p}^2-mE}\sim -C_f\frac{m^2\alpha_{V_s}}{16\pi}\frac{1}{\epsilon},$$

where $D=4+2\epsilon$ and $\mathbf{q}=\mathbf{p}-\mathbf{p}'$. This divergence is absorbed in $D^{(2)}_{d,s}$.

From ultrasoft gluons:

$$\begin{aligned}
\delta G_s &\sim \frac{1}{H_s - E} \int \frac{d^3\mathbf{k}}{(2\pi)^{D-1}} \mathbf{r} \frac{k}{k + H_o - E} \mathbf{r} \frac{1}{H_s - E} \\
&\sim \frac{1}{H_s - E} \mathbf{r} (H_o - E)^3 \left\{ \frac{1}{\epsilon} + \gamma + \ln \frac{(H_o - E)^2}{\nu^2} + C \right\} \mathbf{r} \frac{1}{H_s - E}
\end{aligned}$$

Heavy Quarkonium applications

The Mass ($E_n = -mC_F^2\alpha_s^2/(4n^2)$)

$$M(n,l) = 2m + E_n$$
$$+O(m\alpha_s^3) \quad \text{Billoire}$$
$$+O(m\alpha_s^4) \quad \text{Yndurain, Pineda}$$
$$+O(m\alpha_s^5 \log) \quad \text{Brambilla, Soto, Vairo, Pineda}$$
$$+O(m\alpha_s^5) \text{ (almost)} \quad \text{Kniehl, Penin, Smirnov, Steinhauser}$$
$$+O(mv^4 \times F(mv^2/\Lambda_{QCD})) \quad \text{Voloshin}$$

$$\delta E_{nl}^{NP} = \langle 0|\langle n,l|H_I \frac{1}{E_n - H_8 - H_g} H_I |n,l\rangle|0\rangle \sim \langle \alpha G^2\rangle \left(\frac{1}{mv}\right)^2 \frac{1}{mv^2}\left(1 + \left(\frac{\Lambda_{QCD}}{mv^2}\right)^2 + ...\right).$$

Leading term: Voloshin-Leutwyler; Subleading term: Pineda

Plenty of Observables: **Decay widhts** ($\Gamma(n^3S_1 \to e^+e^-)$, $\Gamma(n^1S_0 \to \gamma\gamma)$), **Bottomonium sum rules. Determination of** m_b. t–$\bar{t}$ **production near threshold. Determination of** m_t. **QED, ...**

Positronium

$$L_{pNRQED} = \int d^3\mathbf{x} d^3\mathbf{X} S^\dagger(\mathbf{x},\mathbf{X},t)$$
$$\left\{ i\partial_0 - \frac{\mathbf{p}^2}{m} + \frac{\alpha}{|\mathbf{x}|} + \frac{\mathbf{p}^4}{4m^3} - \frac{\delta^{(3)}(\mathbf{x})}{m^2}\left(\pi\alpha\left(c_D - 2{c_F}^2\right) + d_s + 3d_v - 16\pi\alpha d_2\right)\right.$$
$$+\frac{\alpha}{2m^2}\frac{1}{|\mathbf{x}|}\left(\mathbf{p}^2 + \frac{1}{\mathbf{x}^2}\mathbf{x}\cdot(\mathbf{x}\cdot\mathbf{p})\mathbf{p}\right) - \frac{\delta^{(3)}(\mathbf{x})}{m^2}\mathbf{S}^2\left(\pi\alpha\frac{4}{3}{c_F}^2 - 2d_v\right)$$
$$\left. -\frac{\alpha}{4m^2}\frac{1}{|\mathbf{x}|^3}\mathbf{L}\cdot\mathbf{S}\left(2c_S + 4c_F\right) - \frac{\alpha{c_F}^2}{4m^2}\frac{1}{|\mathbf{x}|^3}S_{12}(\mathbf{x}) - \delta V(\mathbf{x}) + \mathbf{x}\cdot e\mathbf{E}(\mathbf{X},t)\right\} S(\mathbf{x},\mathbf{X},t)\,.$$

$$\delta V = \frac{\delta^{(3)}(\mathbf{x})}{m^2}\left(\frac{\alpha^2}{3} - \frac{7\alpha^2}{3}\log\mu^2\right) - \frac{7\alpha^2}{6\pi m^2}\mathrm{reg}\frac{1}{|\mathbf{x}|^3}$$

The positronium spectrum can be obtained with $O(m\alpha^5)$ accuracy with this Lagrangian. The cancellation of the scale dependence coming from the different scales involved in the problem is nicely seen.

The calculations can be performed using dimensional regularization.

$$
\begin{aligned}
E_{n,l,j} = 2m - m\frac{\alpha^2}{4n^2} + \frac{m\alpha^4}{8}\Big\{ & -\frac{4}{n^3(2l+1)} + \frac{11}{8n^4} \\
& -\frac{2\alpha}{3\pi}\frac{\delta_{l0}}{n^3}\left(9\log\alpha + 7\log n + 8\log R(n,l) - 14\log 2\right. \\
& \qquad \left. -\frac{49}{15} - 7\left(\sum_{k=1}^{n}\frac{1}{k} + \frac{n-1}{2n}\right)\right) \\
& -\frac{16\alpha}{3\pi}\frac{1-\delta_{l0}}{n^3}\left(\log R(n,l) + \frac{7}{16}\frac{1}{l(l+1)(2l+1)}\right) \\
& +\frac{14}{3}\frac{\delta_{l0}\delta_{s1}}{n^3}\left\{1 + \frac{3\alpha}{7\pi}\left(-\frac{32}{9} - 2\log 2\right)\right\} \\
& +\frac{(1-\delta_{l0})\delta_{s1}}{l(2l+1)(l+1)n^3}\,C_{j,l}\Big\}\,,
\end{aligned}
$$

where $\log R(n,l) = \log\frac{2\langle E_{n,l}\rangle}{m\alpha^2}$ is called the Bethe logarithm and

$$
C_{j,l} = \begin{cases} -\dfrac{l+1}{2\,l-1}\left(2(3l-1) + \dfrac{\alpha}{\pi}(4\,l-1)\right) & , j = l-1\,, \\ -2 - \dfrac{\alpha}{\pi} & , j = l\,, \\ \dfrac{l}{2\,l+3}\left(2(3l+4) + \dfrac{\alpha}{\pi}(4\,l+5)\right) & , j = l+1\,. \end{cases}
$$

QED

Similar techniques. So far, most of the work done for purely leptonic systems. positronium, muonium...

Much better measurements can now be obtained using laser spectroscopy.

High precision measurements can provide tests of new physics. The paradigm is the decay of orthopositronium for which some experiments give values far of the theoretical ones. The theoretical precision is

$$\delta\Gamma/\Gamma^{(0)} \sim O(\alpha^3 \log \alpha)$$

These last results have been obtained using effective field theory methods.
$O(\alpha^2)$ Czarnecki, Melnikov, Yelkhovsky; Adkins, Fell, Sapirstein
$O(\alpha^3 \log \alpha)$ Hill, Lepage; Kniehl, Penin; Melnikov, Yelkhovsky.
($O(\alpha^3 \log^2 \alpha)$ known time ago. Karshenboim)

Some splittings of Positronium also seem to be problematic, for which, more or less, an equivalent level of precision has been achieved.

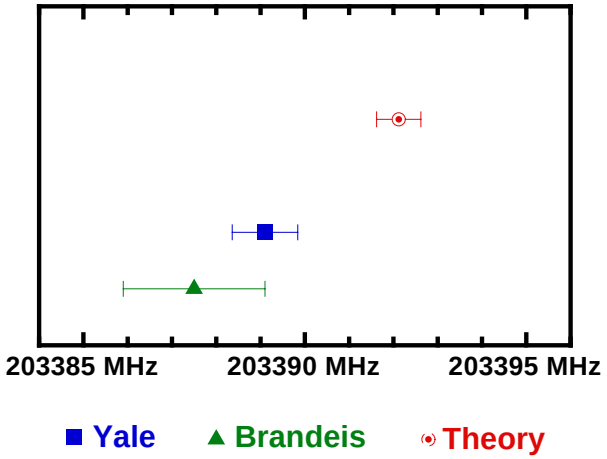

Figure 1: hyperfine splitting of 1S in positronium. From Karshenboim, hep-ph/0201241.

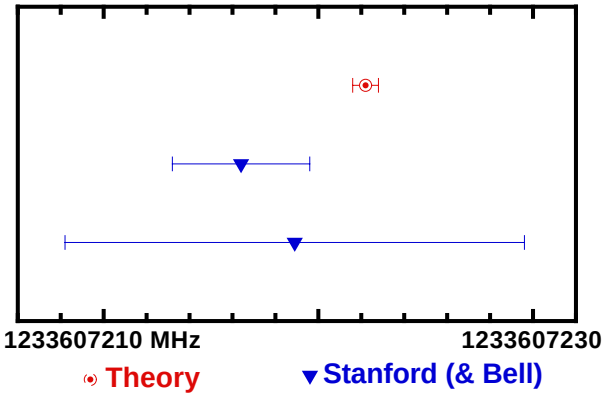

Figure 2: 1S-2S interval in positronium. From Karshenboim, hep-ph/0201241.

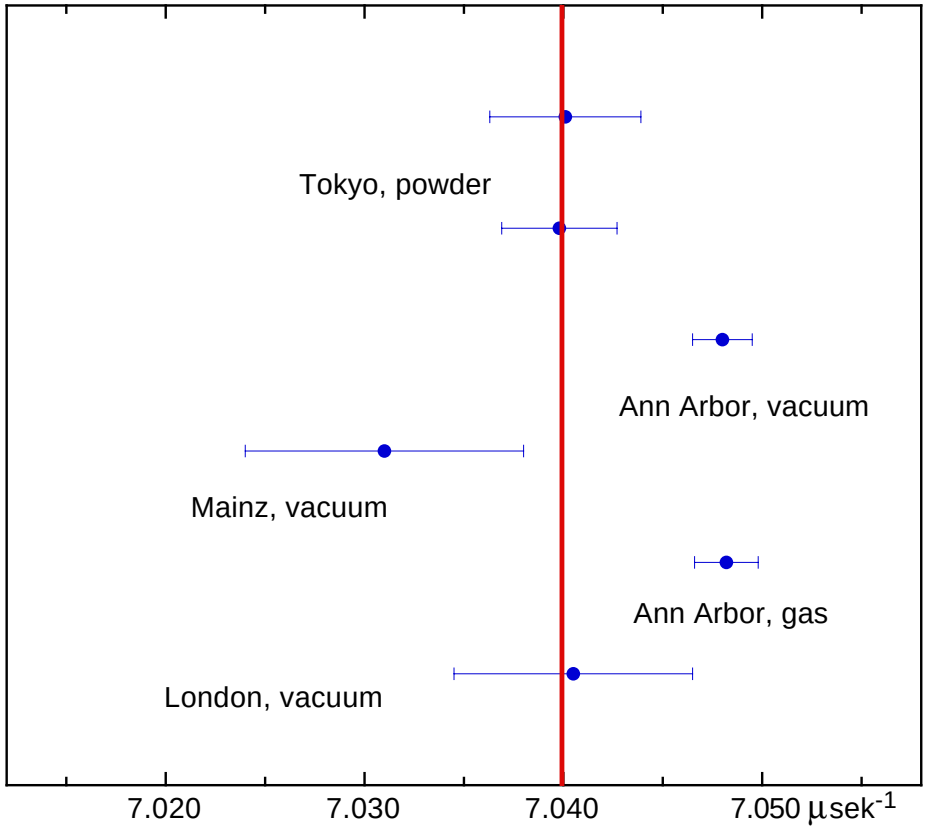

Figure 3: Decay of orthopositronium. From Karshenboim, hep-ph/0201241.

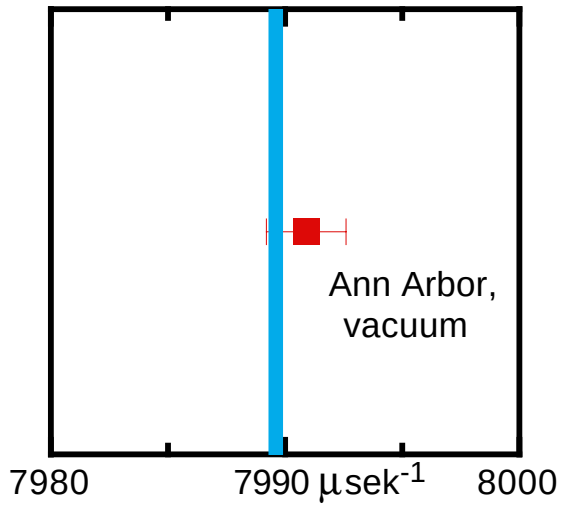

Figure 4: Decay of parapositronium. From Karshenboim, hep-ph/0201241.

QED+hadronic physics

QED+χPT $\longrightarrow$ pionium, ...

QED+HBET $\longrightarrow$ hydrogen, muonic hydrogen, pionic hydrogen

QED+nuclear effective theory $\longrightarrow$ atomic physics

Leading chiral logs to the hyperfine splitting

Connecting particle physics with atomic physics and nuclear physics.

$$\text{HBET} \rightarrow (\text{QED}) \rightarrow \text{NRQED} \rightarrow \text{pNRQED}.$$

$$m_\pi \rightarrow m_e \rightarrow m_e\alpha \rightarrow m_e\alpha^2.$$

$$\delta\mathcal{L} = \frac{c_{3,NR}^{pl_i}}{m_p^2} N_p^\dagger N_p \; l_i^\dagger l_i - \frac{c_{4,NR}^{pl_i}}{m_p^2} N_p^\dagger \boldsymbol{\sigma} N_p \; l_i^\dagger \boldsymbol{\sigma} l_i \,,$$

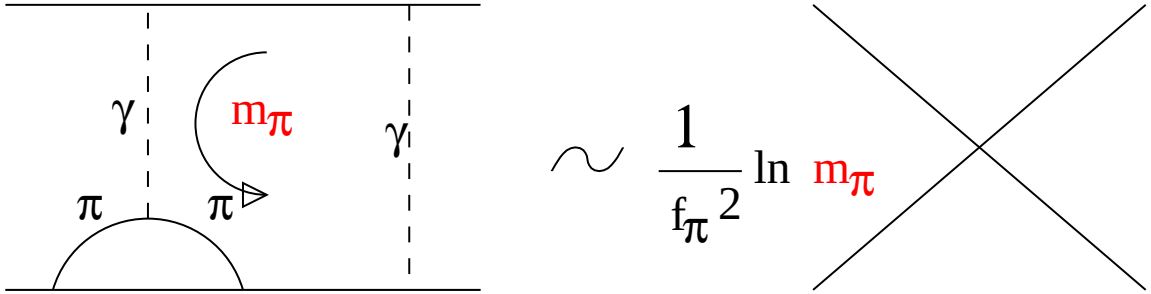

$$\sim \frac{1}{f_\pi{}^2} \ln m_\pi$$

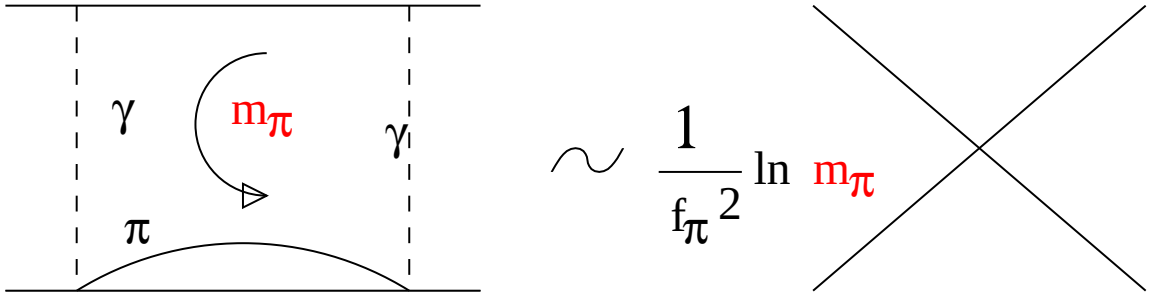

$$\sim \frac{1}{f_\pi{}^2} \ln m_\pi$$

$$\delta V = 2\frac{c_{4,NR}}{m_p^2} \mathbf{S}^2 \delta^{(3)}(\mathbf{r}) \,.$$

$$\delta c_{4,NR}^{pl} \simeq \left(1-\frac{\mu_p^2}{4}\right)\alpha^2 \ln\frac{m_l^2}{\nu^2} + \frac{b_{1,F}^2}{18}\alpha^2 \ln\frac{\Delta^2}{\nu^2} + \frac{m_p^2}{(4\pi F_0)^2}\alpha^2\frac{2}{3}\left(\frac{2}{3}+\frac{7}{2\pi^2}\right)\pi^2 g_A^2 \ln\frac{m_\pi^2}{\nu^2}$$
$$+\frac{m_p^2}{(4\pi F_0)^2}\alpha^2\frac{8}{27}\left(\frac{5}{3}-\frac{7}{\pi^2}\right)\pi^2 g_{\pi N\Delta}^2 \ln\frac{\Delta^2}{\nu^2}\,,$$

$$\delta c_{4,NR}^{pl}(N_c\to\infty) \simeq \alpha^2 \ln\frac{m_l^2}{\nu^2} + \frac{m_p^2}{(4\pi F_0)^2}\alpha^2\pi^2 g_A^2 \ln\frac{m_\pi^2}{\nu^2}\,.$$

$$E_{\rm HF} = 4\frac{c_{4,NR}^{pl_i}}{m_p^2}\frac{1}{\pi}(\mu_{l_i p}\alpha)^3 \sim m_{l_i}\alpha^5\frac{m_{l_i}^2}{m_p^2}\times(\ln m_q, \ln\Delta, \ln m_{l_i})\,.$$

By fixing the scale $\nu = m_\rho$ one obtains the following result for the SU(2) case:

$$E_{\rm HF,logs}(m_\rho) = 4\frac{c_{4,NR}^{pl}(m_\rho)}{m_p^2}\frac{1}{\pi}(\mu_{l_i p}\alpha)^3 = -0.031\ \text{MHz}\,.$$

It predicts around 2/3 of the difference between theory and experiment:

$$E_{\rm HF}(QED) - E_{\rm HF}(exp) = -0.046\ \text{MHz}.$$

The quiral structure of the proton radius and the Lamb shift.

The proton radius is not a well defined object at $O(\alpha^2)$. It can be understood within the effective theory as a Wilson coefficient and be obtained from the (muonic) hydrogen Lamb shift measurent, PSI.

Motivation

Motivation

t–$\bar{t}$ near threshold production region: $E_{cm} \simeq 340 - 360$ GeV. Nonrelativistic system

$$v_{top} = \sqrt{1 - \frac{4m_t^2}{s}} \ll 1$$

$$m_t \gg m_t v_{top} \gg m_t v_{top}^2$$

$$\frac{\alpha_s}{v_{top}} \sim 1 \rightarrow \text{Coulomb resummation} \rightarrow \text{Schroedinger equation}$$

$$\text{LO} \sim \sum_{n=0}^{\infty} c_n \frac{\alpha_s^n}{v_{top}^n}$$

$$\text{NLO} \sim \sum_{n=0}^{\infty} c_n \frac{\alpha_s^n}{v_{top}^n} \times (\alpha_s, v_{top})$$

$$\ldots\ldots$$

Motivation

t–$\bar{t}$ near threshold production region: $E_{cm} \simeq 340 - 360$ GeV. Nonrelativistic system

$$v_{top} = \sqrt{1 - \frac{4m_t^2}{s}} \ll 1$$

$$m_t \gg m_t v_{top} \gg m_t v_{top}^2$$

$$\frac{\alpha_s}{v_{top}} \sim 1 \rightarrow \text{Coulomb resummation} \rightarrow \text{Schroedinger equation}$$

$$\text{LL} \sim \sum_{n=0}^{\infty} c_n \frac{\alpha_s^n}{v_{top}^n} \sum_{m=0}^{\infty} d_m \alpha_s^m \ln^m v$$

$$\text{NLL} \sim \sum_{n=0}^{\infty} c_n \frac{\alpha_s^n}{v_{top}^n} \sum_{m=0}^{\infty} d_m \alpha_s^m \ln^m v \times (\alpha_s, v_{top})$$

$$\ldots\ldots$$

Motivation

t–$\bar{t}$ near threshold production region: $E_{cm} \simeq 340 - 360$ GeV. Nonrelativistic system

$$v_{top} = \sqrt{1 - \frac{4m_t^2}{s}} \ll 1$$

$$m_t \gg m_t v_{top} \gg m_t v_{top}^2$$

$$\frac{\alpha_s}{v_{top}} \sim 1 \rightarrow \text{Coulomb resummation} \rightarrow \text{Schroedinger equation}$$

$$\text{LL} \sim \sum_{n=0}^{\infty} c_n \frac{\alpha_s^n}{v_{top}^n} \sum_{m=0}^{\infty} d_m \alpha_s^m \ln^m v$$

$$\text{NLL} \sim \sum_{n=0}^{\infty} c_n \frac{\alpha_s^n}{v_{top}^n} \sum_{m=0}^{\infty} d_m \alpha_s^m \ln^m v \times (\alpha_s, v_{top})$$

$$\cdots\cdots$$

Summing logs in non-relativistic systems

Large logs understood as ratios of scales: $\ln(mv/m) \sim \ln \alpha_s$, $\ln(mv^2/(mv)) \sim \ln \alpha_s$.
Resummation of logs: $(\alpha_s \ln)^n$.

$$\begin{aligned}
\delta E &\sim m\alpha_s^4 + m\alpha_s^5 \ln \alpha_s + m\alpha_s^6 \ln^2 \alpha_s + \cdots \\
\Gamma(V_Q(nS) \rightarrow e^+e^-) &\sim m\alpha_s^3(1 + \alpha_s^2 \ln \alpha_s + \alpha_s^3 \ln^2 \alpha_s + \cdots) \\
\Gamma(P_Q(nS) \rightarrow \gamma\gamma) &\sim m\alpha_s^3(1 + \alpha_s^2 \ln \alpha_s + \alpha_s^3 \ln^2 \alpha_s + \cdots)
\end{aligned}$$

Nonrelativistic Sum rules (b-$\bar{b}$, c-$\bar{c}$), t-$\bar{t}$ production near threshold

Determination of m_b, m_t, α_s, Higgs-top yukawa coupling, ...

$$J^\mu = \bar{Q}\gamma^\mu Q = B_1 \psi^\dagger \boldsymbol{\sigma} \chi + \cdots ,$$

$$B_1 = 1 + a_1 \alpha_s + a_2 \alpha_s^2 + \cdots$$

B_1 at NNLO: Hoang(QED); Beneke, Signer, Smirnov; Czarnecki, Melnikov
B_1, B_0 at NLL: Pineda; Hoang, Stewart
B_1/B_0 at NNLL: Penin, Pineda, Smirnov, Steinhauser
B_1, B_0 at NNLL (partial): Pineda, Signer

$$(q_\mu q_\nu - g_{\mu\nu})\Pi(q^2) = i \int d^4x e^{iqx} \langle \mathrm{vac}|J_\mu(x) J_\nu(0)|\mathrm{vac}\rangle$$

$$\Pi(q^2) \sim B_1^2 \langle \mathbf{r}=\mathbf{0}| \frac{1}{E-H} |\mathbf{r}=\mathbf{0}\rangle$$

$$G(0,0,E) = \sum_{m=0}^{\infty} \frac{|\phi_{0m}(0)|^2}{E_{0m} - E + i\epsilon - i\Gamma_t} + \frac{1}{\pi} \int_0^\infty dE' \frac{|\phi_{0E'}(0)|^2}{E_{0E'} - E + i\epsilon - i\Gamma_t}$$

A NNLL renormalization group improved expression of $M(V_Q(nS))$ is also needed in order to obtain expressions for the t-$\bar{t}$ production near threshold with NNLL accuracy:
$M(V_Q(nS))$ at NNLL: Pineda; Hoang, Stewart
$M(V_Q(nS)) - M(P_Q(nS))$ at NNNLL: Kniehl, Penin, Pineda, Smirnov, Steinhauser

Relation of the vacuum polarization with $\sigma_{t\bar{t}}$, non-relativistic sum rules and $\Gamma(V_Q(nS) \to e^+e^-)$

$$\Gamma(V \to e^+e^-) \sim \frac{1}{m^2} B_1^2 |\phi(\mathbf{0})|^2$$

$$\sigma_{t-\bar{t}} \sim B_1(\nu)^2 \mathrm{Im} G(0,0,\sqrt{s}) + \cdots$$

$$M_n \equiv \frac{12\pi^2 e_b^2}{n!} \left(\frac{d}{dq^2}\right)^n \Pi(q^2)|_{q^2=0} = \int_0^\infty \frac{ds}{s^{n+1}} R_{b\bar{b}}(s),$$

$$M_n = 48\pi e_b^2 N_c \int_{-\infty}^{\infty} \frac{dE}{(E+2m_b)^{2n+3}} \left(B_1^2 - B_1 d_1 \frac{E}{3m_b}\right) \mathrm{Im}\, G(0,0,E)$$

The top mass

Next Linear Collider. $\delta m_t(\text{exp.}) \lesssim 30$ MeV; decay width 2%: Martinez-Miquel

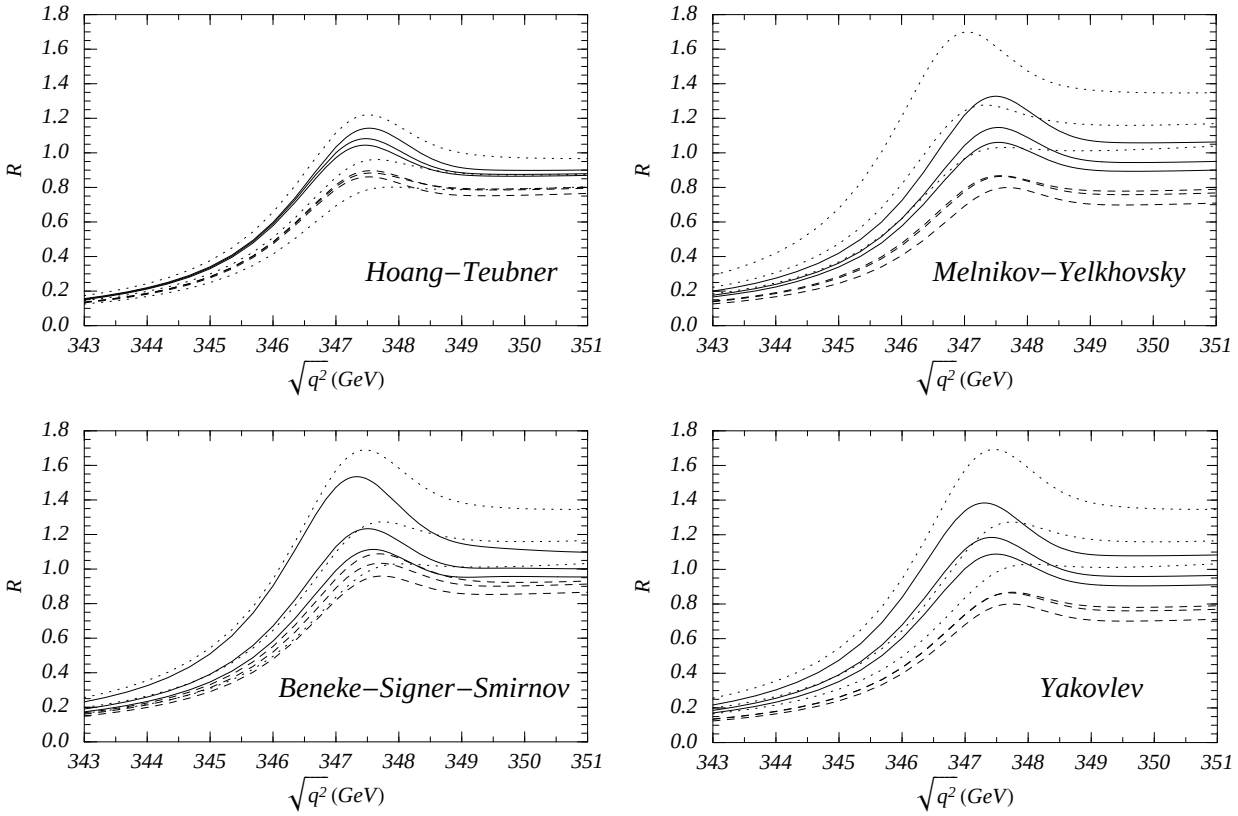

Figure 5:

Total normalized photon induced $t\bar{t}$ cross section at the Internation Linear Collider versus the center of mass energy at LO (dotted line), NLO (dashed line) and NNLO (solid line). Hoang-Teubner used the 1S scheme with $m_t^{1S} = 173.68$ GeV, Melnikov–Yelkhovsky the kinetic mass $m^{\text{kin}}_{t,15\,\text{GeV}} = 173.10$ GeV, and Beneke–Signer–Smirnov and Yakovlev the PS mass $m^{\text{PS}}_{t,20\,\text{GeV}} = 173.30$ GeV. Plot from hep-ph/0001286.

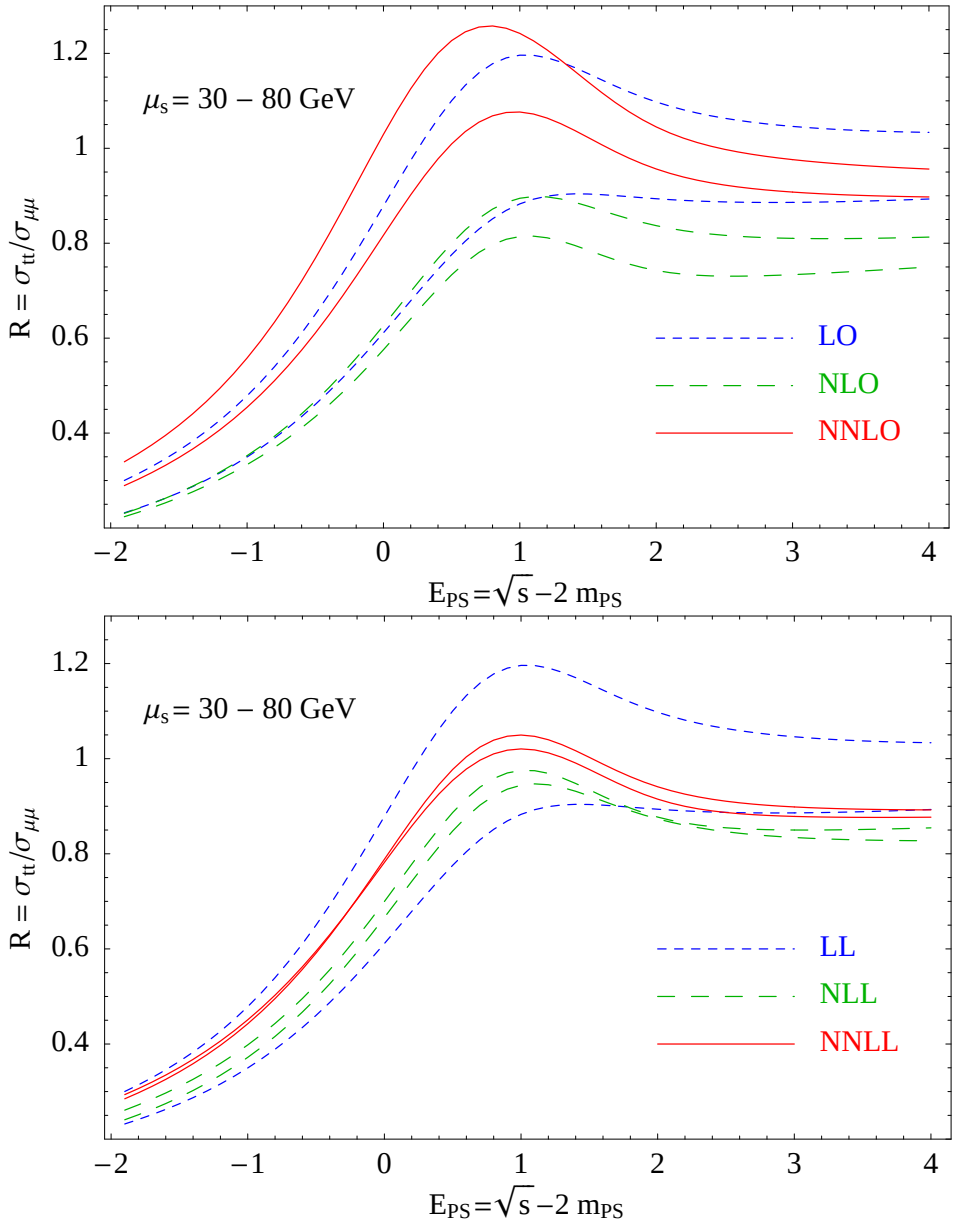

Figure 6: Threshold scan for $t\bar{t}$ using the PS mass, $m_{\rm PS}(20\,{\rm GeV}) = 175$ GeV. The upper panel shows the fixed order results, LO, NLO and NNLO, whereas in the lower panel the RGI results LL, NLL and NNLL are displayed. The soft scale is varied from μ_s=30 GeV to μ_s=80 GeV. Pineda-Signer

The RGI significantly reduces the scale dependence and improves the convergence.

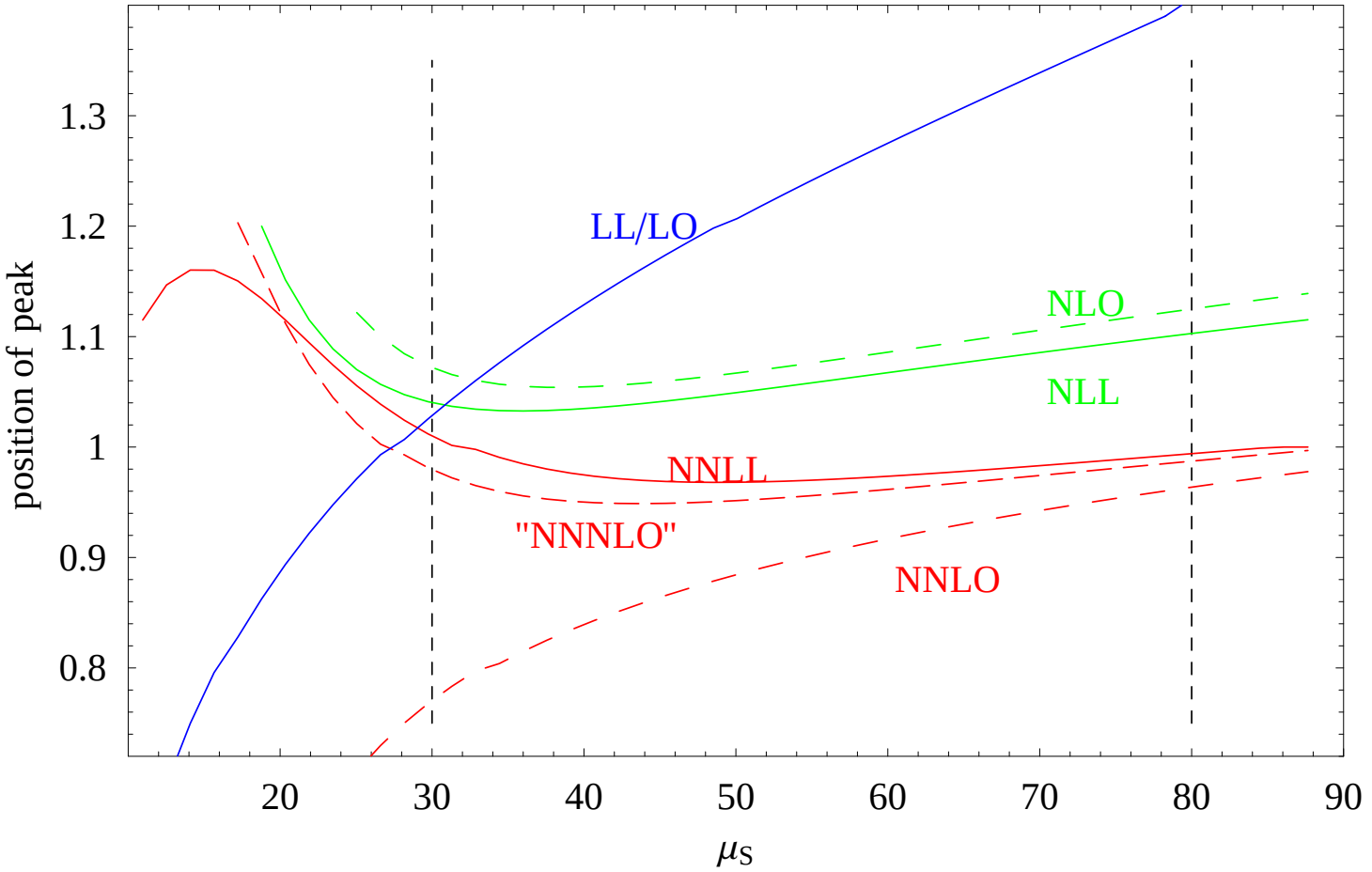

Figure 7: The position of the peak of the RGI threshold cross section as a function of the soft scale μ_s. The vertical dashed lines show the limits of variation used in Figure 6.

Contrary to previous claims, to get an improved determination of the top mass RGI has to be used (or "NNNLO").

Leading logs seem to give the dominant contribution

Strong scale dependence for scales below 30 GeV

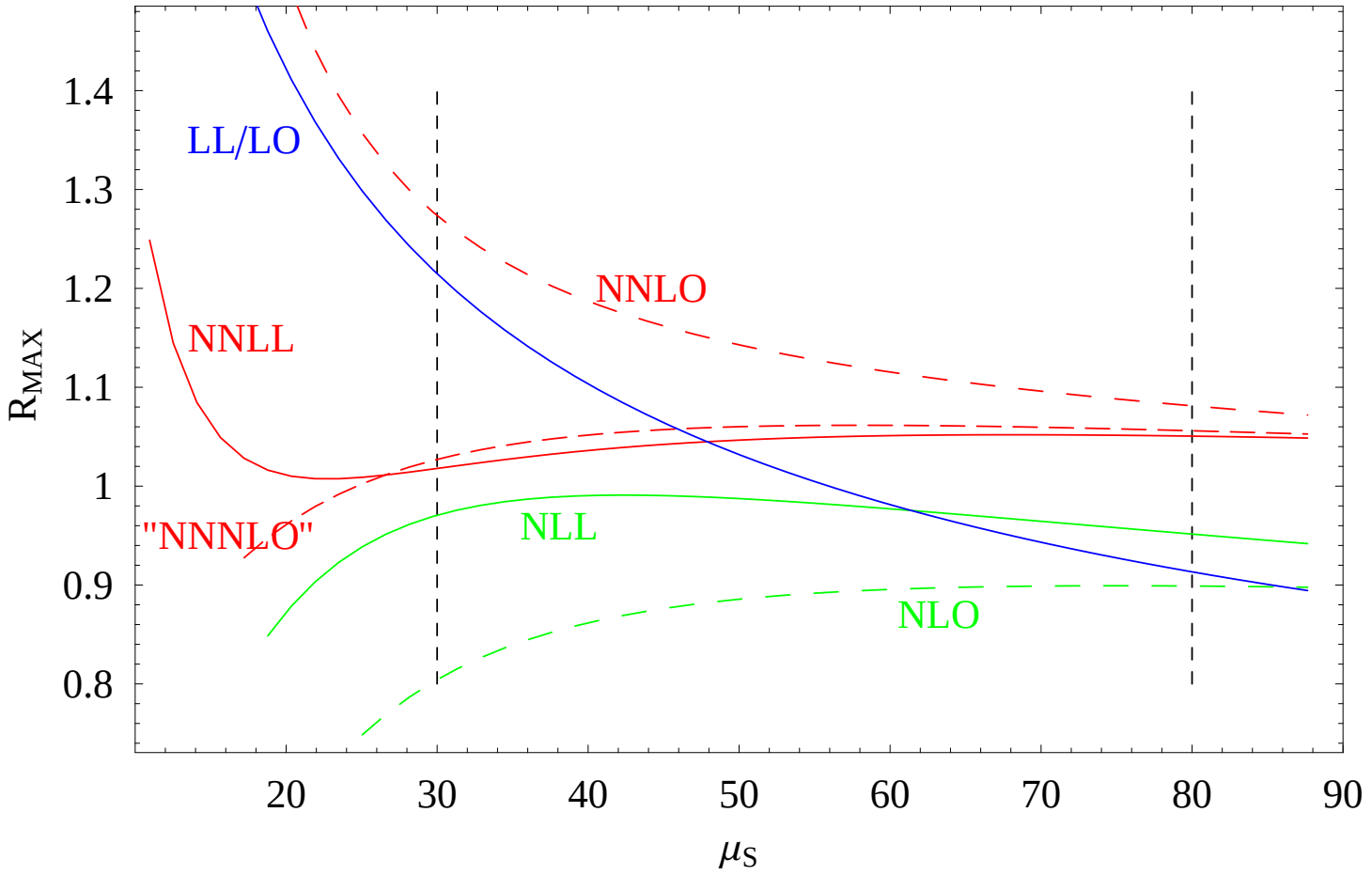

Figure 8: The normalization of the peak of the RGI threshold cross section as a function of the soft scale μ_s. The vertical dashed lines show the limits of variation used in Figure 6.

To get an improved determination of the normalization the RGI is compulsory (NLL and NNLL).

Leading logs seem to give the dominant contribution

Strong scale dependence for scales below 30 GeV

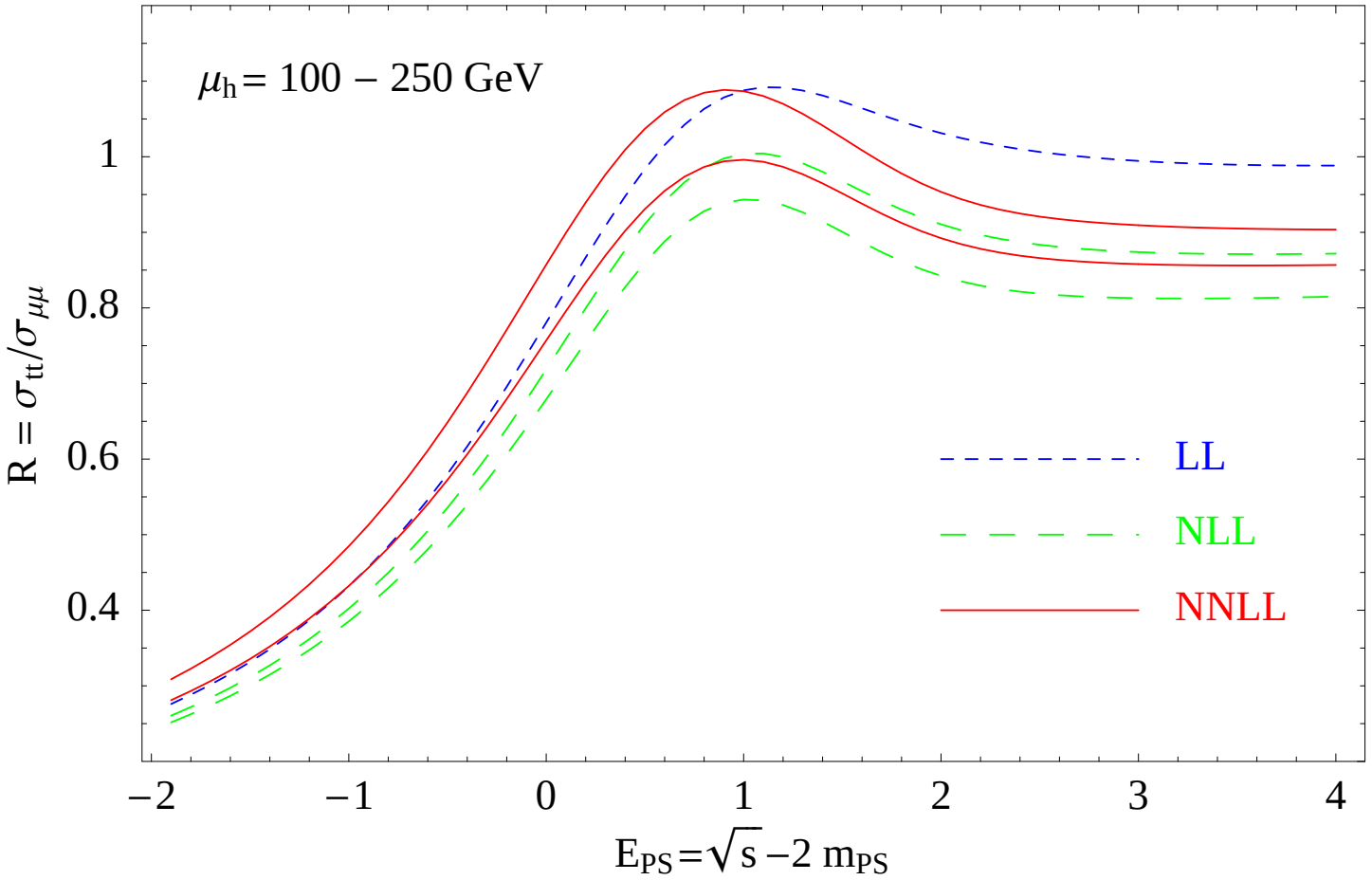

Figure 9: Dependence of the $t\bar{t}$ threshold scan on the hard scale μ_h, using the PS mass. At NNLL (NLL) the lower (upper) curve corresponds to $\mu_h = 250$ GeV, whereas the upper (lower) curve corresponds to $\mu_h = 100$ GeV. Pineda-Signer

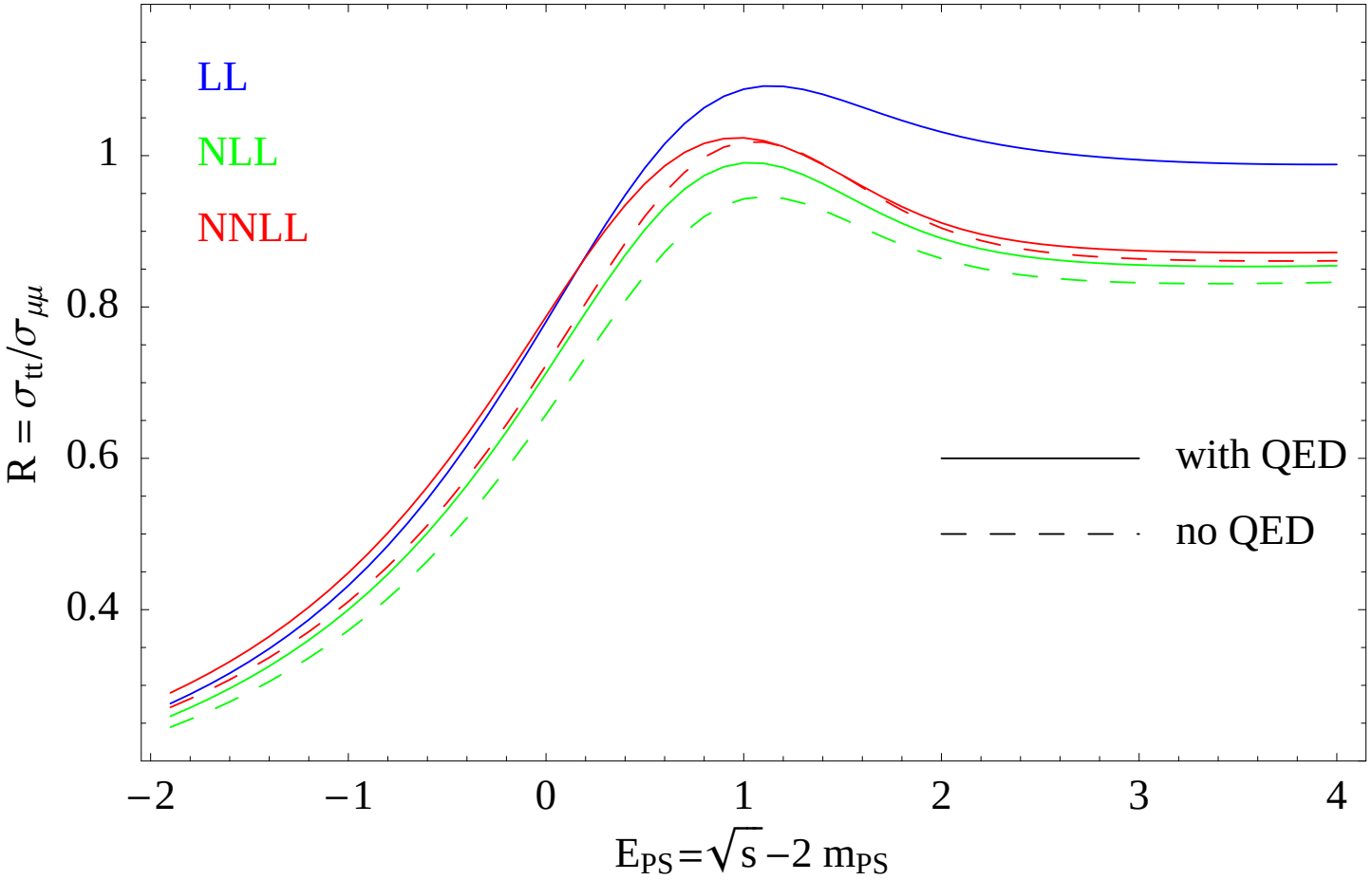

Figure 10: Effects of the QED corrections to the $t\bar{t}$ threshold scan. The hard ans soft sales are chosen as $\mu_h = m_{\rm PS} = 175$ GeV and $\mu_s = 40$ GeV. Pineda-Signer

Error on top mass (position of the peak): ~ 100 MeV

Error on the normalization of the total cross section: $\sim 10\%$

Decay Ratio at NNLL

Penin, Smirnov, Steinhauser, Pineda

$$\frac{\Gamma(V_Q(nS)\to e^+e^-)}{\Gamma(P_Q(nS)\to\gamma\gamma)} \sim 1+\alpha\ln\alpha+\alpha^2\ln^2\alpha+\cdots$$
$$+\alpha+\alpha^2\ln\alpha+\alpha^3\ln^2\alpha+\cdots$$
$$+\alpha^2+\alpha^3\ln\alpha+\alpha^4\ln^2\alpha+\cdots$$

$$\frac{\Gamma(T(1S)\to e^+e^-)}{\Gamma(\eta_t(1S)\to\gamma\gamma)} = \frac{1}{3Q_t^2}\left(1-0.13198-0.0179492\right) .$$

$$\frac{\Gamma(\Upsilon(1S)\to e^+e^-)}{\Gamma(\eta_b(1S)\to\gamma\gamma)} = \frac{1}{3Q_b^2}\left(1-0.302-0.111\right) .$$

$$\Gamma(\eta_b(1S)\to\gamma\gamma) = 0.659\pm 0.089(\text{th.})^{+0.019}_{-0.018}(\delta\alpha_s)\pm 0.015(\text{exp.})\ \text{KeV} ,$$

$$\frac{\Gamma(oPs \to 3\gamma)}{\Gamma(pPs \to 2\gamma)} = \frac{4(\pi^2-9)}{9\pi}\alpha\left\{1+\left(5-\frac{\pi^2}{4}+A_o\right)\frac{\alpha}{\pi}+\frac{7}{3}\alpha^2\ln\alpha\right.$$
$$+\left[\left(5-\frac{\pi^2}{4}\right)^2+\left(5-\frac{\pi^2}{4}\right)A_o+B_o-B_p\right]\left(\frac{\alpha}{\pi}\right)^2$$
$$-\left[-\frac{73}{9}-\frac{7\,A_o}{3}+\frac{7\,\pi^2}{12}+2\,\log(2)\right]\frac{\alpha^3}{\pi}\ln\alpha$$
$$\left.+\frac{83}{36}\alpha^4\ln^2\alpha-\frac{7}{6\pi}\alpha^5\ln^3\alpha+\cdots\right\},$$

where $A_o = 10.286606(10)$, $B_o = 44.87(26)$ and $B_p = 5.1243(33)$.

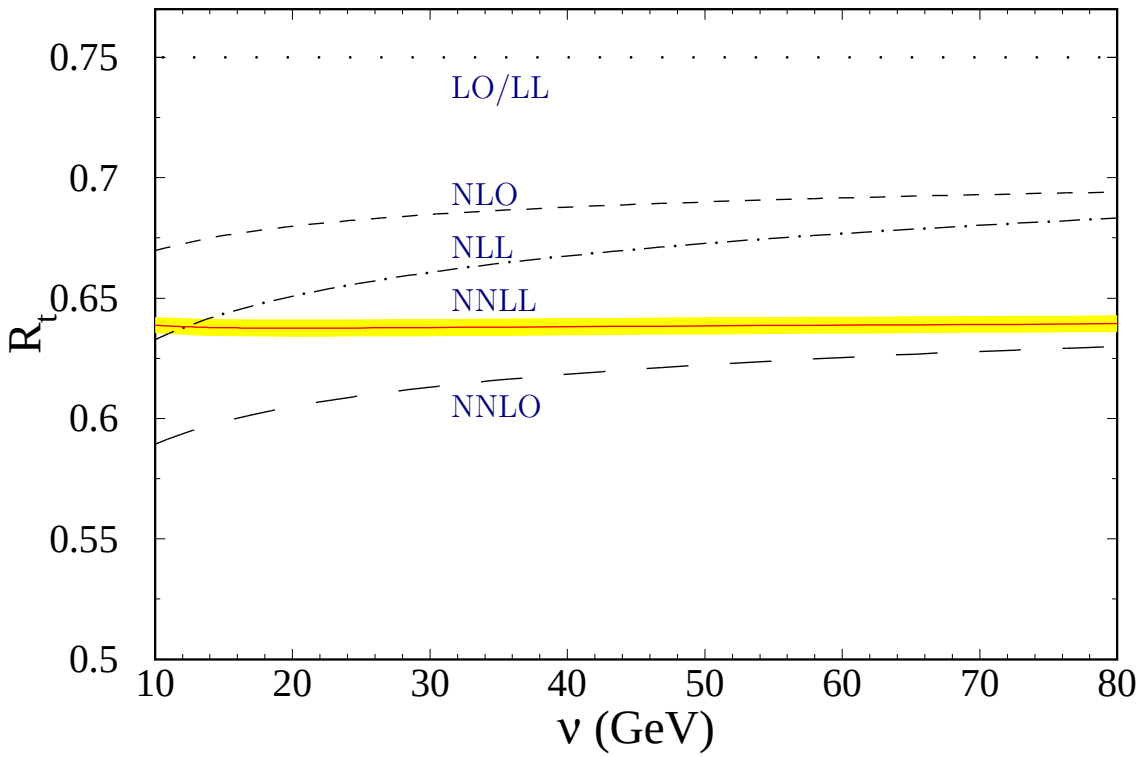

Figure 11: The spin ratio as the function of the renormalization scale ν in LO (dotted line), NLO (short-dashed line), NNLO (long-dashed line), LL (dotted line), NLL (dot-dashed line), and NNLL (bold solid line) approximation for the (would be) toponium ground state with $\nu_h = m_t$. For the NNLL result the band reflects the errors due to $\alpha_s(M_Z) = 0.118 \pm 0.003$

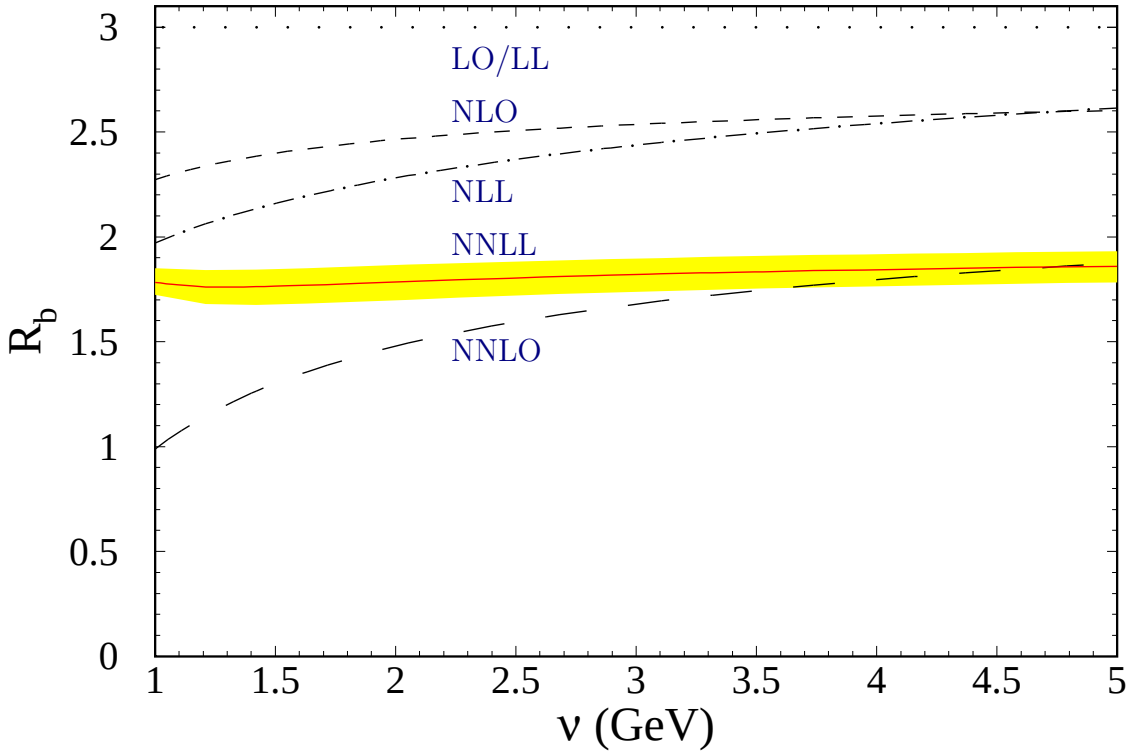

Figure 12: The spin ratio as the function of the renormalization scale ν in LO (dotted line), NLO (short-dashed line), NNLO (long-dashed line), LL (dotted line), NLL (dot-dashed line), and NNLL (bold solid line) approximation for the bottomonium ground state with $\nu_h = m_b$. For the NNLL result the band reflects the errors due to $\alpha_s(M_Z) = 0.118 \pm 0.003$

Inclusive electromagnetic decays: bottomonium

Pineda-Signer

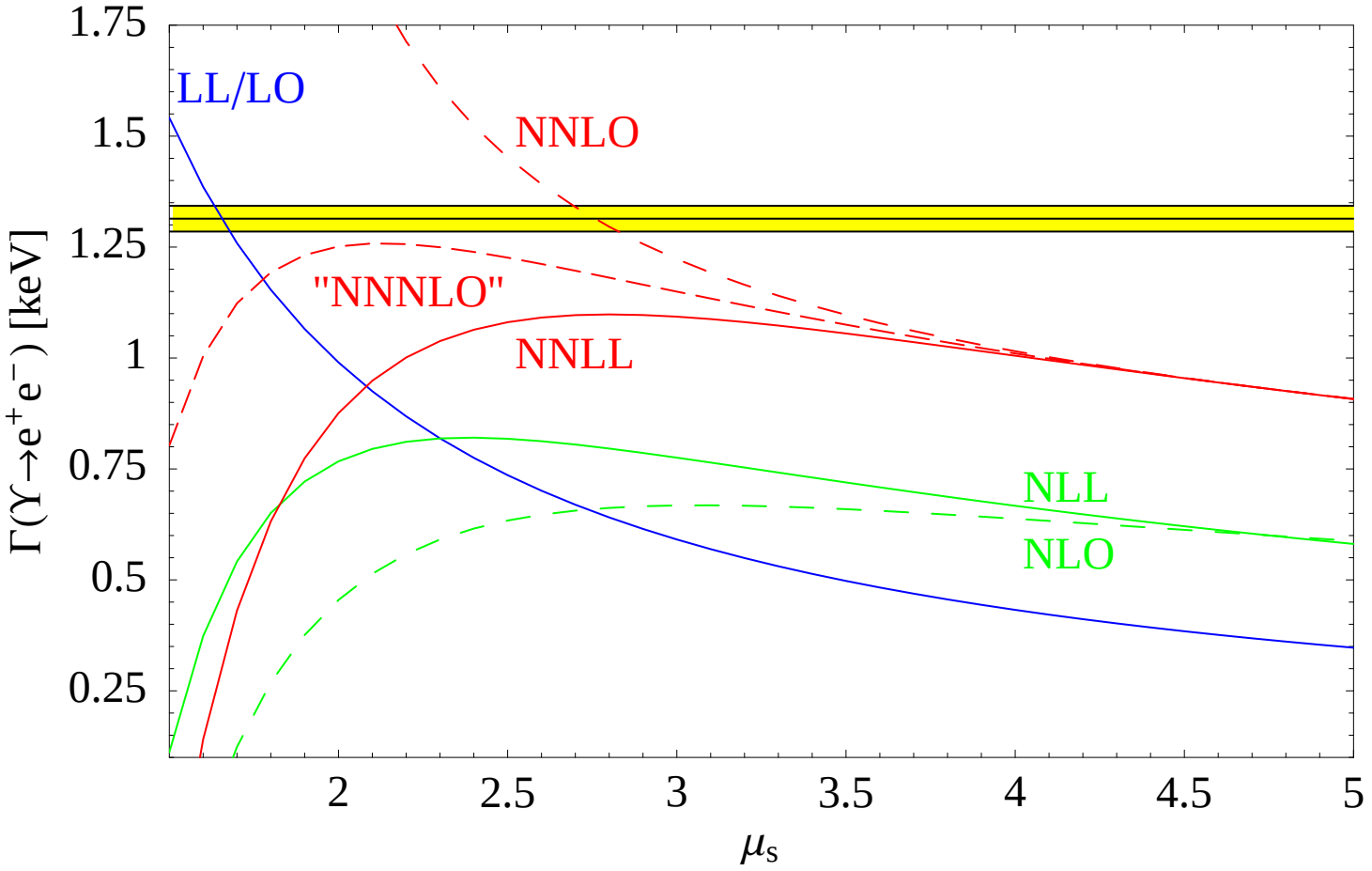

Figure 13: Prediction for the $\Upsilon(1S)$ decay rate to e^+e^-. We work in the RS' scheme.

The effect of the resummation of logarithms is important if compared with just keeping the single logarithm.

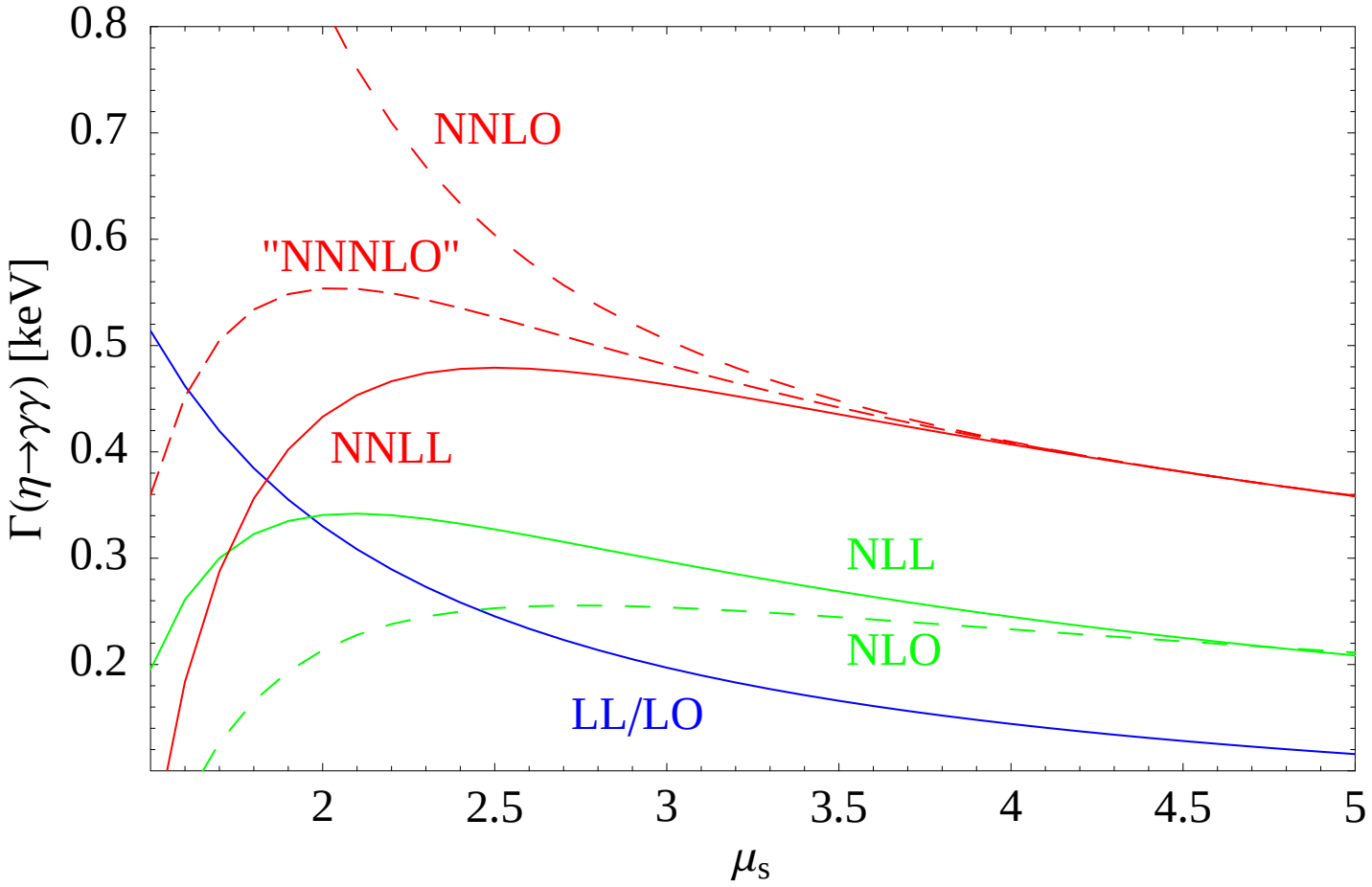

Figure 14: Prediction for the $\eta_b(1S)$ decay rate to two photons. We work in the RS' scheme.

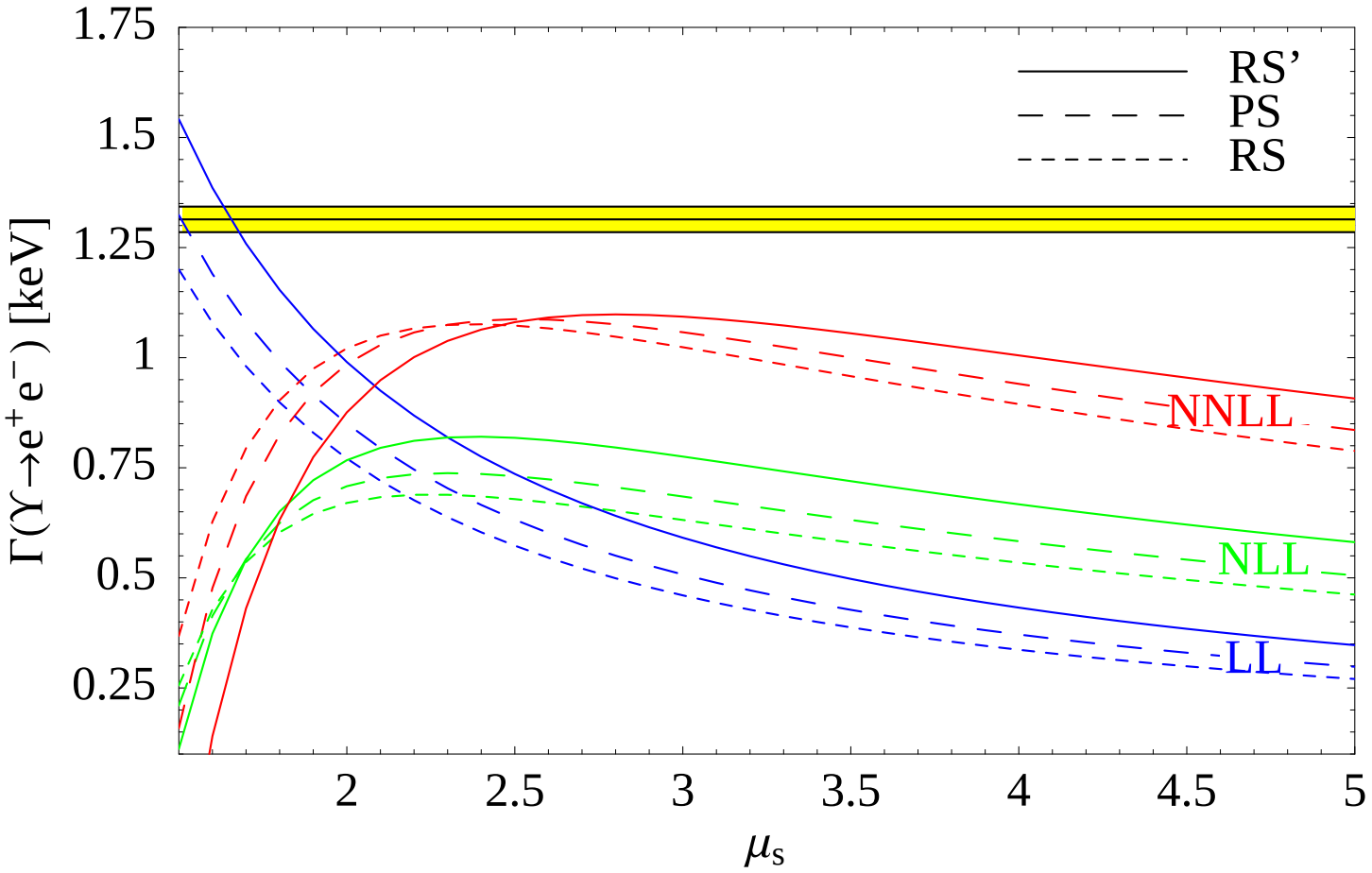

Figure 15: Prediction for the $\Upsilon(1S)$ decay rate to e^+e^- at LL, NLL and NNLL for the PS, RS and RS' mass.

The effects due to the change of scheme are small. Other sources of error are much larger.

Non-relativistic Sum rules: bottomonium

Pineda-Signer

$$M_n \equiv \frac{12\pi^2 e_b^2}{n!}\left(\frac{d}{dq^2}\right)^n \Pi(q^2)|_{q^2=0} = \int_0^\infty \frac{ds}{s^{n+1}} R_{b\bar{b}}(s),$$

$$M_n = 48\pi e_b^2 N_c \int_{-\infty}^{\infty} \frac{dE}{(E+2m_b)^{2n+3}}\left(B_1^2 - B_1 d_1 \frac{E}{3m_b}\right) \mathrm{Im}\, G(0,0,E)$$

n	$m_{b,\mathrm{PS}}(2\ \mathrm{GeV})$	Δ_{th}	Δ_{exp}	Δ_α	Δ_{tot}	$\overline{m}_b$
6	4460	40	50	35	70	4135 ± 65
8	4505	45	25	30	60	4170 ± 55
10	4515	45	15	25	55	4185 ± 50
12	4520	45	10	20	50	4185 ± 45
14	4520	40	10	15	45	4185 ± 40
n	$m_{b,\mathrm{RS}}(2\ \mathrm{GeV})$	Δ_{th}	Δ_{exp}	Δ_α	Δ_{tot}	$\overline{m}_b$
6	4315	55	50	25	80	4140 ± 70
8	4360	65	30	20	75	4180 ± 65
10	4370	65	20	10	70	4190 ± 60
12	4370	65	15	5	65	4190 ± 60
14	4370	65	10	5	65	4185 ± 55

Table 1: *Extraction of $m_{b,\mathrm{PS/RS}}(2\ GeV)$ with errors for various n. All values are given in MeV and rounded to 5 MeV. The total error has been obtained by adding the partial errors in quadrature. The corresponding value for the $\overline{\mathrm{MS}}$ mass with its error is given in the last column.*

small $n \longrightarrow$ larger experimental error (not to use theoretical ansatz above threshold for experiment)

Large $n \longrightarrow$ larger theoretical error, bad convergence of the perturbative series (it also depends on the scheme).

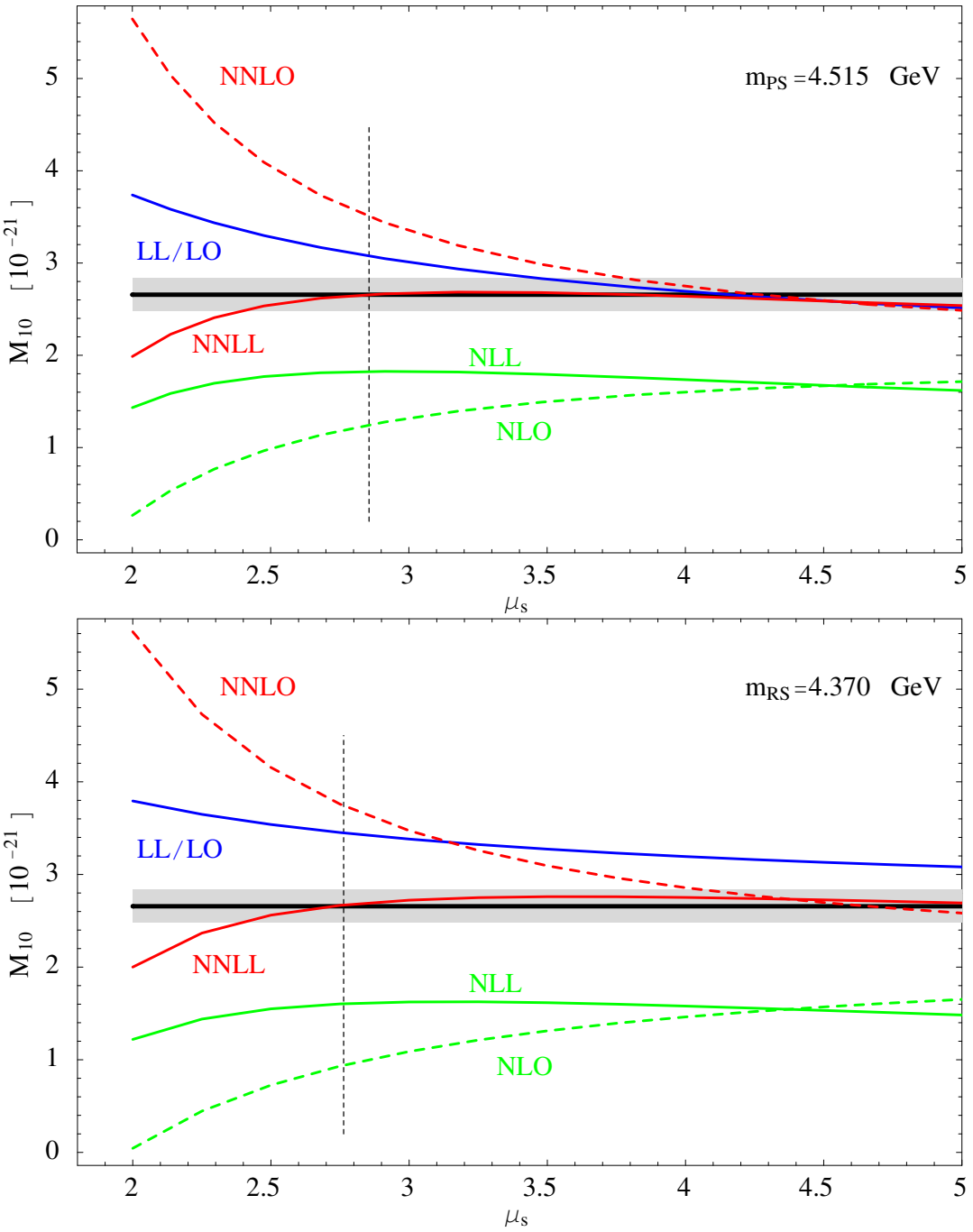

Figure 16: *The moment M_{10} as a function of μ_s at LO/LL, NLO, NLL, NNLO and NNLL for $m_{b\mathrm{PS}}(2\ \mathrm{GeV}) = 4.515\ \mathrm{GeV}$ in the PS scheme (upper figure), and for $m_{b\mathrm{RS}}(2\ \mathrm{GeV}) = 4.370\ \mathrm{GeV}$ in the RS scheme (lower figure). The experimental moment with its error is also shown (grey band).*

$$m_{b,\mathrm{PS}}(2\mathrm{GeV}) = 4.52 \pm 0.06 \ \mathrm{GeV},$$
$$m_{b,\mathrm{RS}}(2\mathrm{GeV}) = 4.37 \pm 0.07 \ \mathrm{GeV}.$$

$$\overline{m}_b(\overline{m}_b) = 4.19 \pm 0.06 \, \mathrm{GeV}.$$

The perturbative series is sign-alternating. This is the opposite than for electromagnetic decays. The convergence of the perturbative series in sum rules is also better in sum rules than for electromagnetic decays.

NNLO determinations of the bottom sum rules suffer from very huge theoretical uncertainties (which are not always incorporated in the errors): bad scale dependence and bad convergence of the perturbative series. Therefore, they can not provide precise determinations of the bottom mass.

Conclusions

The use of Effective Field Theories has lead us to a better understanding of the dynamics of NR systems.

A rigorous connection between Quantum Field Theories and a NR Quantum-mechanical formulation of the NR systems now exists for both the perturbative and nonperturbative case.

It is now understood how to perform calculations in dimensional regularization.

Power counting is now better understood.

$$\overline{m}_b(\overline{m}_b) = 4.19 \pm 0.06\,\mathrm{GeV}.$$

Error on top mass (position of the peak): ~ 100 MeV

Error on the normalization of the total cross section: $\sim 10\%$